Impacts of Emission Policies in China on Air Pollution and Human Health

by

Mingwei Li

B.Eng., Tsinghua University (2010)
M.Eng., Tsinghua University (2013)

Submitted to the Department of Earth, Atmospheric and Planetary Sciences
in partial fulfillment of the requirements for the degree of

Doctor of Philosophy in Atmospheric Chemistry

at the

MASSACHUSETTS INSTITUTE OF TECHNOLOGY

June 2019

Signature redacted

Author...   ....
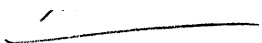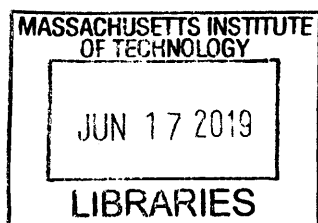Department of Earth, Atmospheric and Planetary Sciences
May 24, 2019

Signature redacted

Certified by.....................................   ....
Noelle Eckley Selin
Associate Professor in the Institute of Data, Systems and Society, and Department of Earth,
Atmospheric and Planetary Sciences
Thesis Supervisor

Signature redacted

Accepted by................   ....
Robert D. van der Hilst
Schlumberger Professor of Earth and Planetary Sciences
Head, Department of Earth, Atmospheric and Planetary Sciences

Impacts of Emission Policies in China on Air Pollution and Human Health

by

Mingwei Li

Submitted to the Department of Earth, Atmospheric and Planetary Sciences
on May 24, 2019, in partial fulfillment of
the requirements for the degree of
Doctor of Philosophy in Atmospheric Chemistry

ABSTRACT

Precursor emissions of air pollution can be reduced at emitting sources by end-of-pipe control policies or as co-benefits of climate policies that limit fossil fuel. Identifying cost-effective control strategies requires understanding policy costs, chemical non-linearities in pollution formation, and the value of health benefits. China suffers from severe air pollution, and is implementing both policies, but relevant studies are limited. This thesis incorporates three studies that examine the air quality co-benefits of China's recent climate policy for China and transboundary countries, and the potential changes in the sensitivities of inorganic $PM_{2.5}$ to precursor emissions in China. The first study quantifies co-benefits of China's climate policy from reducing $PM_{2.5}$ using a modeling framework that couples an energy-economic model with sub-national detail for China (C-REM) and an atmospheric chemical transport model GEOS-Chem. The effects of an illustrative climate policy, a price on CO_2 emissions, are simulated under three stringencies. In a policy scenario consistent with China's recent pledge to peak CO_2 emissions by 2030 (the 4% Policy scenario), national health co-benefits from improved $PM_{2.5}$ pollution can partially or fully offset policy costs depending on chosen health valuation. This study also suggests co-benefits would rise with increasing policy stringency. Using the same model simulations, the second study further compares co-benefits from $PM_{2.5}$ and ozone in China and three downwind countries (South Korea, Japan and the United States). This study suggests that under the 4% Policy scenario, avoided premature deaths from reducing ozone are about half of those from $PM_{2.5}$ in China, and the total avoided deaths in transboundary countries are about 4% of those in China. The third study examines the potential changes in the sensitivities of inorganic $PM_{2.5}$ to precursor emissions in China in response to the current and projected national reductions in SO_2 and NO_x emissions. Under scenarios that reduce SO_2 and NO_x emissions, sensitivities to SO_2 and NO_x emissions would increase, but sensitivity to NH_3 emissions would decrease in January and July. The largest absolute changes in sensitivities are found in January for NO_x and NH_3.

Thesis Supervisor: Noelle Eckley Selin
Title: Associate Professor in the Institute of Data, Systems and Society, and Department of Earth, Atmospheric and Planetary Sciences

Acknowledgments

First of all, I would like to thank my PhD advisor Professor Noelle Selin. Over the past six years, she supported my research interests, connected me with collaborators, provided timely feedbacks, and guided my research to a comprehensive level. I feel extremely lucky to have her as a role model for a scientist and a mentor.

I am very grateful for having the chance to work closely with Professor Valerie Karplus. Her group developed the energy-economic model that I used throughout my thesis, and she provided tremendous help with all the projects in this thesis.

It is my great honor to have Professor Susan Solomon on my thesis committee. I really appreciate her scientific insights, research advice, and support, which would be valuable for my entire academic career. I would also like to acknowledge my thesis committee member Professor Andrew Babbin. As a marine biogeochemist, he led me to think from new perspectives.

I would like to thank the Selin group and the Karplus group. My thesis is inspired by earlier research from group members, and I received a lot of help from them. Especially, I would like to thank my co-authors Da Zhang, Chiao-Ting Li, and Kathleen Mulvaney. I also would like to thank Shaojie Song, who helped me in many aspects during the past years.

I also appreciate the long-term support from my parents and the company from all the friends I made in my PhD. Special thanks go to my partner Dr. Lu Shen. Without his support, I cannot put together this thesis.

Contents

List of Figures

9

List of Tables

Chapter 1 Introduction

1.1 Motivation

$PM_{2.5}$ (fine particulate matter with a diameter less than or equal to 2.5 μm) and ozone are two major air pollutants that are harmful to human health. $PM_{2.5}$ are fine solid or liquid particulates suspended in the atmosphere, and can penetrate deep into human's lungs and circulatory systems through breathing. Long-term exposure to $PM_{2.5}$ can cause respiratory and cardiovascular diseases, leading to premature mortality (e.g. Burnett et al., 2014). Ambient ozone has been found to contribute to risk of respiratory mortality (e.g. Jerrett et al., 2009), and recently circulatory mortality (Turner et al., 2016). Lelieveld et al. (2015) estimated that $PM_{2.5}$ and ozone are responsible for 3.15 (1.52—4.60) and 0.14 (0.09—0.21) million premature deaths, respectively in 2010 worldwide.

Ozone and the majority of $PM_{2.5}$ are chemically formed in the atmosphere from gaseous precursors that are emitted mainly from anthropogenic sources. Particulates are a mixture of chemical components including sulfate, nitrate, ammonium, black carbon (BC), and organic carbon. They can be emitted directly from combustion, such as BC emissions from trucks. However, a larger portion of $PM_{2.5}$ is chemically formed from gaseous precursors, including inorganic $PM_{2.5}$ and secondary organic carbon. Inorganic $PM_{2.5}$, namely sulfate, nitrate, and ammonium, are chemically linked and formed from sulfur dioxide (SO_2), nitrogen oxides (NO_x), and ammonia (NH_3). Ozone is also a secondary air pollutant which is formed from photochemical reactions of NO_x, carbon monoxide (CO), and volatile organic compounds (VOCs) in the presence of sunlight. Combustion of fossil fuels, particularly coal, in power plans and industrial boilers is a major source of SO_2, NO_x, and CO. NO_x and CO can also be emitted from vehicles. By contrast, NH_3 mostly comes from agricultural activities including fertilizer and livestock waste, and the majority of VOCs is emitted naturally from vegetation.

Besides air pollution, climate change is another major threat to sustainability. Addressing climate change requires deep cuts in global CO_2 emissions, which originate from many of the same fossil fuel combustion processes that are responsible for the emissions of air pollutants.

Therefore, climate policies that limit CO_2 emissions can simultaneously reduce emissions of air pollutants and their precursors, resulting in co-benefits from mitigating air pollution and associated health impacts.

China's dense population and high coal share in energy consumption make it the world's leading GHG emitter and home to severe air pollution (van Donkelaar et al., 2016; Ma et al., 2017). Air pollutants and their precursors from China can also travel long distances, contributing to $PM_{2.5}$ and ozone concentrations in downwind countries including South Korea, Japan, and the US. Under the 2015 Paris Agreement, many developing nations have pledged to control domestic GHG emissions. Specifically, China has committed to achieve a peak in national CO_2 emissions and to increase its non-fossil share of primary energy to 20% by 2030. Co-benefits on air quality are expected to be large. Limited air quality co-benefits studies in China (He et al., 2010; West et al., 2013; Peng et al., 2018) did not consider how policy dynamically shapes the evolution of the energy system, and did not conduct an economic cost and health benefit analysis. Although climate policies are not necessarily the most cost-effective air pollution control strategies for China, co-benefits form an important basis for coordinating air quality and climate policy when the latter is binding. In addition, previous studies often omitted co-benefits from reducing ozone, and did not quantified co-benefits of China's carbon policy on transboundary regions.

Long before carbon policies, China has enforced end-of-pipe regulations to control air pollutants, which has led to a large reduction in SO_2 emissions since 2006 and a small reduction in NO_x emissions since 2012 (Zhao et al., 2013; Zheng et al., 2018). Since inorganic $PM_{2.5}$ is formed through complex and non-linear chemical processes from its precursors—SO_2, NO_x, and NH_3, previous studies have examined how inorganic $PM_{2.5}$ responds to changes in emissions of each precursor, i.e. sensitivity of $PM_{2.5}$ to emissions, to help better design pollution control policies (e.g. Ansari and Pandis, 1998; Pinder et al., 2007). Studies focusing on China suggested a larger sensitivity to NH_3 emissions, but comparisons to the three precursors varied by season and by region (Wang et al., 2011; Kharol et al., 2013; Lee et al., 2015). In addition, sensitivities have been found to change as a result in large-scale emission reductions through altering the chemical regime of nitrate formation and levels of oxidants in the US (Holt et al.,

2015). As China's SO_2 and NO_x emissions continue to decrease, sensitivities of inorganic $PM_{2.5}$ to further emission reductions could change.

This thesis examines the impacts of emission policies in China on air pollution and human health and addresses the following questions:

(1) How large are the air quality co-benefits of China's recent climate policy? How do the monetized health co-benefits in China compare with policy cost?

(2) How large are the co-benefits of China's climate policy for other countries affected by China's air pollution?

(3) How would sensitivities of inorganic $PM_{2.5}$ to precursor emissions change in response to changes in anthropogenic emissions in China?

1.2 Chapter Descriptions

Chapter 2 Co-benefits of China's climate policy from reducing fine particulate matter

This chapter is based on Li et al. (2018), and quantifies air quality co-benefits of China's recent climate policy by reducing $PM_{2.5}$ using a model framework that couples an energy-economic model with sub-national detail for China (C-REM) and an atmospheric chemical transport model GEOS-Chem. The effects of an illustrative climate policy, a price on CO_2 emissions, are simulated under three stringencies. Co-benefits on human health associated with reduced $PM_{2.5}$ are further monetized, and are compared to the economic costs of climate policies. In a policy scenario consistent with China's recent pledge to peak CO_2 emissions by 2030, national health co-benefits can partially or fully offset policy costs depending on chosen health valuation. This study also suggests co-benefits would rise with increasing policy stringency.

Chapter 3 Co-benefits of China's climate policy for air quality and human health in China and transboundary regions

This chapter is adapted from Li et al. (2019) that is currently under review in *Environmental Research Letters*. Using the same modeling framework as in Chapter 2, this chapter further

compares the co-benefits of China's climate policy on both $PM_{2.5}$ and ozone in China to those in three downwind countries (South Korea, Japan and the United States). Avoided premature deaths from reducing ozone are about half of those from $PM_{2.5}$ in China, and the total avoided deaths in transboundary countries are about 4% of those in China. Total avoided deaths in South Korea and Japan are dominated by reductions in $PM_{2.5}$-related mortality, but ozone plays a more important role in the US. Similar to co-benefits for $PM_{2.5}$ in China, co-benefits for ozone and for both pollutants in those downwind countries also rise with increasing policy stringency.

Chapter 4 Potential changes in the sensitivities of inorganic fine particulate matter to precursor emissions in China

This chapter examines the potential changes in the sensitivities of inorganic $PM_{2.5}$ to precursor emissions in China in response to national reductions in SO_2 and NO_x emissions. Anthropogenic emissions of SO_2 and NO_x are predicted from C-REM, and inorganic $PM_{2.5}$ is simulated using GEOS-Chem. Sensitivities are derived from simulations with 10% perturbations in emissions of each precursor nationally. We find that inorganic $PM_{2.5}$ in 2010 is most sensitive to NH_3 emissions in January and more sensitive to SO_2 and NO_x emissions in July. Under scenarios that reduce SO_2 and NO_x emissions, sensitivities to SO_2 and NO_x emissions would increase, but sensitivity to NH_3 emissions would decrease in January and July. The largest absolute changes in sensitivities are found in January for NO_x and NH_3.

Chapter 2 Air quality co-benefits of China's climate policy from reducing fine particulate matter

Abstract

Climate policies targeting energy-related CO_2 emissions, which act on a global scale over long time horizons, can result in localized, near-term reductions in air pollution and adverse human health impacts. Focusing on China, the largest energy using and CO_2 emitting nation, we develop a cross-scale modeling approach to quantify these air quality co-benefits, and compare them to climate policy's economic costs. We simulate the effects of an illustrative climate policy, a price on CO_2 emissions. In a policy scenario consistent with China's recent pledge to peak CO_2 emissions by 2030, we project that national health co-benefits from improved air quality rise with increasing policy stringency and can partially or fully offset policy costs depending on chosen health valuation.

2.1 Introduction

Advancing environmental sustainability in systems with multiple interacting natural and human components is a major scientific and analytical challenge. Climate change and local air quality are two threats to sustainability that offer significant potential for co-control (Aunan et al., 2004; Shindell et al., 2012; McCollum et al., 2013; West et al., 2013), because emissions of CO_2, the major energy-linked greenhouse gas (GHG), originate from many of the same combustion processes responsible for emissions of air pollutants. Efforts to identify co-control opportunities are complicated by the difficulty of simulating how policy acts across space and time and interacts with complex, and often nonlinear, relationships among economic activity, emissions, ambient air quality and human health.

Addressing climate change will require deep cuts in global emissions of CO_2 and other GHGs. Many developing nations, including China, have pledged to control domestic GHG emissions

under the 2015 Paris Agreement (China National Development and Reform Commission, 2015). These efforts interact with a broader set of non-target sustainability challenges (Nemet et al., 2010), among them air quality. Degraded air quality is an immediate, often localized environmental burden and a leading cause of mortality (Vos et al. 2015). Here we focus on these interactions in China. China's high coal share makes it the world's leading GHG emitter and home to severe local pollution. While climate policy does not necessarily trigger the most cost-effective air pollution control strategies, co-benefits form an important basis for coordinating air quality and climate policy when the latter is binding.

Among climate change policy studies, several have focused on co-benefits (West et al. 2013; Parry et al., 2015). Co-benefits are outcomes not directly targeted by policy, including reductions in non-targeted pollutants (Dong et al., 2015), changes in air quality (Thompson et al., 2014), reduced adverse health outcomes (Shindell et al., 2012) and avoided economic costs (Nielsen and Ho, 2013). In the United States, Thompson et al. (2014) found large but rapidly diminishing co-benefits with increasing climate policy stringency. Shindell et al. (2016) showed that CO_2 reductions in the United States that are consistent with a 2°C global target would deliver near-term benefits that would probably exceed policy costs.

Co-benefits studies for China have largely focused on the impacts of climate or air pollution policies on national and, in a few cases, provincial emissions. In a model that captures pollution abatement costs, Nam et al. (2013) evaluated the SO_2 reduction target in China's Eleventh Five Year Plan (2006–2010), and found that non-target reductions in CO_2 exceeded the stringency of a concurrent carbon intensity target. Dong et al. (2015) used a provincial economic model of China to predict energy consumption, and applied an optimization tool to select cost-effective carbon mitigation and air pollutant mitigation technologies and estimate CO_2 and air pollution emissions in 2030. They found that well-developed regions see only marginal co-benefits in terms of reduced air pollutant emissions, while provinces that are large energy users or are relatively coal- or industry-intensive obtain larger co-benefits.

A few China-focused studies have extended policy assessment to air quality, but either omitted or presented only aggregated national health effects, and did not consider how policy dynamically shapes the evolution of the energy system. He et al. (2010) quantified the impact

18

of energy policies in China on air pollution, taking sustainable energy scenarios described in government plans (Zhou et al., 2003) as an input, and focusing on formation of fine particulate matter with a diameter less than or equal to 2.5 μm ($PM_{2.5}$). Nielsen and Ho (2013) simulated the impact of national air pollution policy on energy use, emissions, air quality and public health in a single-region model of China, showing that SO_2 controls during the Eleventh Five-Year Plan (2006–2010) delivered significant public health benefits, while a nationwide CO_2 tax was projected to improve air quality at low cost.

We establish a novel, cross-scale integrated approach to assess co-benefits and costs that captures how policy alters the economy and energy system across spatial scales (here, provincial to national), time horizons (our dynamic energy–economic model captures evolution of the energy system from 2010 to 2030) and as a function of policy ambition. Our analysis captures the contribution of airborne pollution transport, simulating nonlinear relationships among emissions, air quality and health effects, while preserving regional detail, in a self-consistent framework. This integrated co-benefit analysis of a developing country (China) resolves sub-national spatial as well as temporal impacts of policy.

2.2 Methods

To simulate policy impacts and economy–environment interactions, we develop the regional emissions air quality climate and health (REACH) framework, which couples an energy–economic model, the China Regional Energy Model (C-REM), with an atmospheric chemistry model, GEOS-Chem. Using C-REM, we first simulate a CO_2 price, which results in deployment of least-cost CO_2 reduction strategies to meet a CO_2 intensity constraint, and obtain provincial energy use and emissions of CO_2 and air pollutants through to 2030. We model three policy scenarios that target CO_2 intensity reductions of 3%, 4% or 5% per year between 2015 and 2030 (3% Policy, 4% Policy and 5% Policy), and compare them to a No Policy scenario. The 3% Policy simulates a continuation of China's CO_2 intensity reduction commitment prior to the 2015 Paris Agreement; total CO_2 emissions in 2030 are projected to be 13.5 gigatons (Gt). The 4% Policy is consistent with China's recent commitment to halt its rise in CO_2 emissions by 2030 (with projected CO_2 emissions of 11.4 Gt in 2030), achieving a 60–65% reduction in CO_2 intensity by 2030 relative to its 2005 level. The 5% Policy reduces China's CO_2 intensity to the

19

projected world average in 2030 (with projected emissions of 9.7 Gt in 2030), and is comparable to the scenario described by Raftery et al. (2017), which limits the global temperature increase to 2 °C. Emissions factors for each pollutant by province, sector and energy type in 2007 are derived from emissions reported in the Regional Emission Inventory in Asia (REAS; Kurokawa et al., 2013), and are calibrated to 2010 and 2015 based on national total emissions reported in the multi-resolution emission inventory for China (MEIC: http://www.meicmodel.org). To obtain anthropogenic emissions of air pollutants and their precursors in 2030 for each scenario, levels of economic activity or energy use simulated in C-REM are used to scale associated sectoral emissions in 2015 assuming an exponential decay in emissions factors through to 2030 to account for the technology improvement in end-of-pipe controls. These emissions are then input to GEOS-Chem (v. 9-01-03, with a horizontal resolution of $0.5° \times 0.667°$ in East Asia) to simulate $PM_{2.5}$ formation. We then calculate national and provincial monetized health damages from $PM_{2.5}$ using three concentration–response functions and two health valuation methods to examine uncertainties in health co-benefits.

2.2.1 C-REM

C-REM is a global general equilibrium model that resolves China's economy and energy system at the provincial level, including production, consumption, interprovincial and international trade, energy use and emissions of CO_2 and local pollutants (Zhang et al., 2013; Luo et al., 2016). Several previous analyses have used C-REM to evaluate China's energy and climate policy (Springmann et al., 2015; Karplus et al., 2016; D. Zhang et al., 2016). The model represents 30 provinces in mainland China in detail and divides the rest of the world into four regions (United States, Europe, other developing countries and other developed countries). In China, the model represents production, intermediate input flows, consumption, interprovincial trade and energy based on China's Regional Input–Output Tables (for 2007; National Bureau of Statistics of China, 2011a) and Energy Balance Tables (National Bureau of Statistics of China, 2011b). Global energy and economic flows for regions other than China and China's international imports and exports are parameterized using the 8th release of the Global Trade Analysis Project data (GTAP; Narayanan et al., 2012). The primary inputs to production in the dataset include labour, capital and natural resources, with endowments denominated in 2007 US$. To prepare inputs for C-REM, we aggregate commodities into four energy sectors and

nine non-energy composites (Table A.1). Based on general equilibrium theory (Arrow and Debreu, 1954), the model is formulated using the mathematical programming subsystem MPSGE in GAMS (Rutherford, 1999) and solved at five-year intervals through to 2030. A detailed description of the C-REM model structure and assumptions is provided in Zhang et al. (2013) for a static version of the model and Luo et al. (2016) for the dynamic version of the model (with the latter used in the present study). To enable a clear comparison of carbon pricing between the business-as-usual (No Policy) and policy scenarios, without its interactions with other policy and technology uncertainties, we do not explicitly model scenarios that vary assumptions on future technological changes or policies that will affect China's development of non-fossil fuel energy (for example, renewable feed-in-tariff adjustments), natural gas (such as expansion of shale gas usage and increased imports of liquified natural gas) and the electrification of transportation (a subsidy for electric vehicles, for example). To represent ongoing improvements in energy efficiency unrelated to energy price changes, we assume in all scenarios an autonomous energy efficiency improvement rate of 1.7% per year in China following X. Zhang et al. (2016). The autonomous energy efficiency improvement rate is applied to all production sectors and household final demand as an exogenous trend for all provinces. The No Policy scenario through 2015 is calibrated to historical observations (National Bureau of Statistics of China, 2012), while projections for future periods reflect economic growth assumptions in the Thirteenth Five-Year Plan (FYP, 2016-2020) and related documents describing the growth trajectories of individual provinces as discussed in Luo et al (2016). C-REM specifies factor endowments in the base year, labour productivity, and population growth rate, but treats economic responses to policies endogenously. Policy is imposed as a constraint on CO_2 intensity that results in a shadow price on CO_2, increasing the relative cost of CO_2 intensive production. Responses to policy are reflected in changes in sectoral outputs, GDP, and welfare. Elasticity values in constant-elasticity-of-substitution production functions, which are used to represent technologies and define substitution possibilities among inputs, mediate the extent of these adjustments Zhang et al. (2013).

2.2.2 Emissions projections

Provincial-level CO_2 and pollutant emissions are computed based on projected energy use and economic activity, multiplied by emissions factors. We compute emissions factors for CO_2 and

pollutant species SO_2, NO_x, NH_3, BC, and OC in 2007 by province, sector, and energy type. We only consider CO_2 emissions from energy combustion, because China's commitment in the Paris Agreement and related policies are primarily targeted at industry-related CO_2 emissions. CO_2 emissions factors from combustion are estimated following IPCC guidelines (IPCC, 2006). GHG emissions from non-combustion processes are not considered primarily because they are not the focus of the study (to illustrate quantification of co-benefits using the example of energy-related co-benefits of CO_2 mitigation) but also because of a lack of accurate data sources and mitigation cost information for China. On pollutants, we divide provincial pollution quantities reported in the REAS inventory (Kurokawa, et al., 2013) by the corresponding sector energy use (for combustion emissions) or activity level (for non-combustion emissions) in C-REM. To ensure consistency in the attribution of emissions between REAS and C-REM, sectors in REAS are aggregated to match the sectors in C-REM. The aggregation consolidates the detailed energy types in REAS into the four energy sectors in C-REM and maps the industrial sectors in REAS into the four C-REM industrial sectors, which include construction (CON), energy intensive industries (EIS), other manufacturing industries (MAN), and metal/non-metal minerals mining (OMN). Table A.2 illustrates how sectors in REAS are mapped to those in C-REM. For each sector, REAS divides sources into two categories, combustion and non-combustion: for example, 87% of SO_2 comes from combustion sources (mostly due to use of fossil fuel as production input) and 13% from non-combustion sources, while only 0.4% of NH_3 comes from combustion sources and 99.6% from non-combustion sources. For each sector, we associate combustion emissions with energy use by type and the non-combustion emissions to the activity level (projected quantity of economic output). We divide the emissions quantities in REAS by C-REM model outputs in 2007 to yield emissions factors specific to each pollutant for each economic sector and each province in 2007. Emissions factors due to use of coal in the electricity (ELE) sector are generally smaller than in the other industrial sectors, such as MAN, because the ELE sector in China has access to coal of better quality (i.e. higher heating value and lower sulfur content).

To update the REAS emission inventory in 2007 for more recent years, we calibrate the emissions factors for 2010 and 2015 using available data. The calibration in 2010 is conducted by scaling the emissions factors in this particular year to match national totals in the MEIC inventory (http://www.meicmodel.org). An exception is the emissions factor for NH_3, which

we scale to match the data in Streets et al. (2003), and we apply an additional 30% reduction, as recommended by Kharol et al. (2013) to better match observations. The calibration for 2015 is conducted by scaling the emissions factors to match the extrapolated trend for 2015 defined by the observations for 2010 and 2012 in MEIC, since 2015 data are not yet available. Emissions factors for SO_2, NO_x, NH_3, BC, and OC in 2015 are 77%, 72%, 57%, 56% and 53% of their levels in 2007.

To account for technology improvement in end-of-pipe solutions that are exogenous to climate policy in China, we assume that emissions factors in all scenarios continue to decrease after 2015. To simulate the evolution of emissions factors over time, we adopt the methodology in Webster et al. (2008), in which emissions factors are estimated to decline exponentially in time to match the decreasing historical trend observed in 15 developed countries. The trend parameter (exponential decay constant) of each pollutant is listed in Table 2.1. SO_2 has a slightly faster decay rate compared to NO_x and NH_3, reflecting the aggressive deployment of sulfur scrubbers on new power plants. In addition, we assume that the emissions factors related to biomass burning, which contributes significantly to BC and OC, will also have a faster decay rate than other pollutants to represent stricter enforcement of banning the burning of crop residuals in rural areas. This decline in the emissions factors is meant to capture efficiency improvement in end-of-pipe controls for air pollutants, e.g. newer sulfur scrubbers may have better removal efficiency, and not to capture accelerated adoption of tailpipe control technologies by the industry that may be triggered by environmental regulations. Emissions factors (ton SO_2 and NO_x per ton of coal use) in 2030 in our study remain higher than current factors for the U.S. For example, the emissions factor of SO_2 in the electricity sector in 2030 in our study is 10% higher than the aggregate U.S. emissions factor in 2015, and that of NO_x is four times the level of the U.S. in 2015 (US Energy Information Administration, 2017; US Environmental Protection Agency, 2016).

Table 2.1. Trend parameter for emissions factors to decay exponentially over time.

Pollutant Species	Trend Parameter
SO_2	-0.03
NO_x	-0.01
NH_3	-0.015
BC	-0.03
OC	-0.03
Biomass	-0.07

In this study, to isolate co-benefits, we assume that climate policies do not trigger accelerated adoption of end-of-pipe control technologies as policies target only CO_2 emissions. We conducted three additional simulations to examine the sensitivity of emissions in the No Policy scenario to emissions factor changes. First, we keep emissions factors fixed at their 2015 level. A comparison between this simulation and the No Policy scenario is shown in Figure 2.1. Without emissions factors changes, No Policy emissions show large increases: BC is 95% higher, and OC is 140% higher in 2030, reflecting the absence of existing policies aimed at reducing biomass burning in agricultural areas. Other pollutant species also show substantial increases by 2030: 59% for SO_2, 21% for NO_x, and 29% for NH_3. A second and third scenario double and triple, respectively, the emissions decay factors. We find that SO_2 emissions fall by 36% and 58%, NO_x emissions fall by 14% and 25%, NH_3 emissions by 20% and 35%, BC by 26% and 42%, and OC by 13% and 22% in the No Policy scenario by 2030, in the two respective cases.
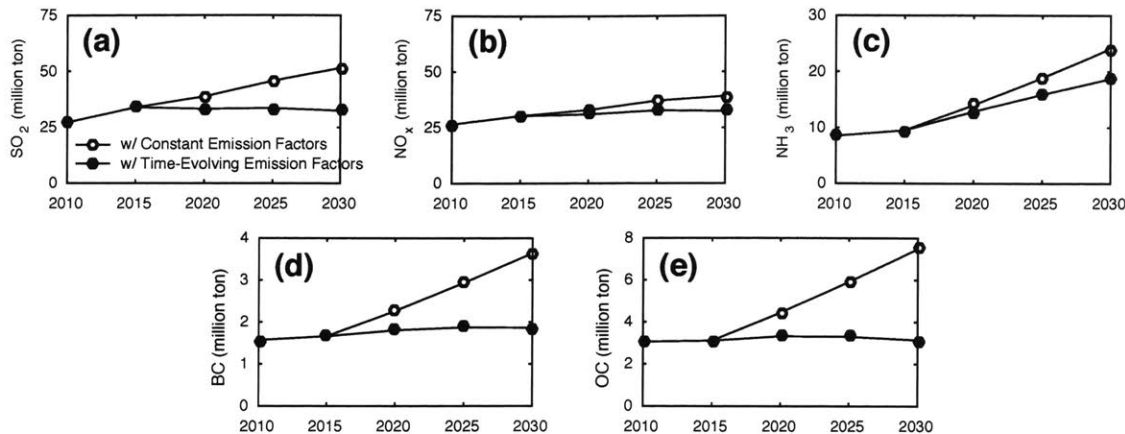
Figure 2.1. Comparison of emissions trajectories with time-evolving emissions factors and constant emissions factors.

2.2.3 GEOS-Chem

GEOS-Chem is a global 3-D chemical transport model driven by assimilated meteorological data from the Goddard Earth Observation System (GEOS) of the NASA Global Modeling and Assimilation Office (GMAO) (http://www.geos-chem.org/). The aerosol simulation in GEOS-Chem represents an external mixture of secondary inorganic aerosols, carbonaceous aerosols, sea salt, and dust aerosols coupled with gas-phase chemistry. For this work, we use version 9-01-03 of GEOS-Chem with a horizontal resolution of $0.5° \times 0.667°$ in East Asia (Wang et al., 2004). It has 47 vertical layers from surface to 80 km with 14 layers in the lowest 2 km and a surface layer of 130 m. For our simulations, we corrected errors in nighttime mixing depth using the methodology suggested in Walker et al (2012). Additionally, we reduce the HNO_3 concentration used as input for thermodynamic gas and particle partitioning by 25% at each time step to avoid the overproduction of nitrate, following Heald et al (2012).

To validate the GEOS-Chem simulation of $PM_{2.5}$, we compiled an observational dataset from available publications which includes annual measurements of sulfate, nitrate, and ammonium, BC, OC, and total $PM_{2.5}$ from 25 sites in China taken between 2005 and 2010 (Zhang et al., 2012; He et al., 2012; Xu et al., 2012; Zhao et al., 2013; Zhang et al., 2013), and compared with simulated concentrations from 2007 or 2010 (whichever year was closer). For sulfate, nitrate, and ammonium aerosols, we obtained additional measurements at 26 sites from the Acid Deposition Monitoring Network in East Asia (EANET) in 2010 (Asia Center for Air Pollution

Research, 2012), 25 of which are outside China but within our simulation domain. GEOS-Chem generally reproduces the spatial distribution of ambient concentrations of different aerosol species with correlation coefficient (r) between annual mean concentrations of model simulations and observations >0.6 (Table 2.2 and Figure 2.2). Simulated sulfate and nitrate aerosols are underestimated by about 30%, and BC and OC are underestimated by about 40%, which altogether contribute to an underestimation of total $PM_{2.5}$ by 13%. The difficulties for atmospheric chemistry models to capture high concentrations of $PM_{2.5}$ especially in urban areas have been discussed extensively in the literature (e.g. Wang et al., 2014), and can be caused by missing emissions, formation pathways such as in the case of secondary organic aerosols (Fu et al., 2012), or spatial heterogeneity in emissions, meteorology, and chemistry. Since the major $PM_{2.5}$ co-benefits we found in this study are within sulfate-nitrate-ammonium aerosols, co-benefits could be underestimated considering these biases in simulated inorganic aerosols. However, these biases are comparable to or better than biases found in other studies which assess nonlinearities in inorganic aerosol chemistry (e.g. Holt et al., 2013; Kharol et al., 2013), and suggest our model is doing as well as possible given the current state of science.

Table 2.2. Correlation coefficient and bias between annual mean concentrations of model and observations.

Species	Correlation (r)	Bias (model-observation)
Sulfate	0.92	-27%
Nitrate	0.79	-31%
Ammonium	0.91	15%
BC	0.74	-44%
OC	0.63	-42%
$PM_{2.5}$	0.68	-13%
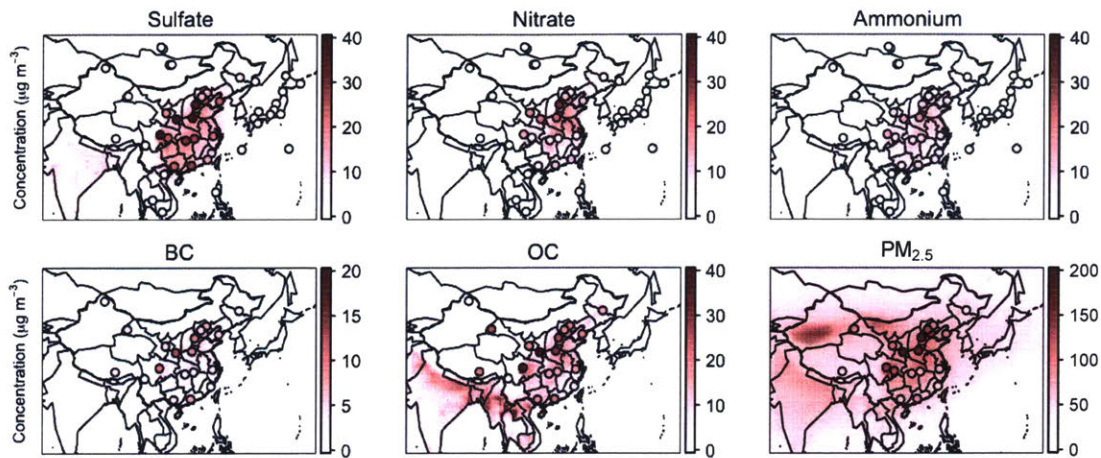
Figure 2.2. Simulated annual mean surface concentrations in East Asia for the year 2010 (sulfate, nitrate, ammonium, BC, OC, and total $PM_{2.5}$). Circles indicate locations and concentrations of measurements used for model comparison.

To calculate air quality co-benefits of climate policies, we conducted five GEOS-Chem simulations; one for the 2010 base year, and four scenarios in 2030 (the No Policy and three climate policy scenarios). Gridded emissions of SO_2, NO_x, BC, and OC in 2010 are generated by scaling gridded REAS emissions in 2007 for each province according to emissions outputs from C-REM model in 2007 and 2010. As mentioned above, we use gridded emissions of NH_3 in 2000 from Streets et al. (2003) with a 30% reduction (Kharol et al., 2013) as gridded emissions in 2010. Gridded emissions in 2030 for all scenarios are scaled by province based on emission outputs from C-REM in 2010 and 2030 as described above, reflecting changes in economic structure and patterns of energy use as they evolve over time and adjust in response to policy. The spatial distribution of emissions within provinces does not change over time.

Each simulation is one year long with a six-month spin-up period, and the same meteorological fields for the year 2010 are used in all simulations. We alter only the anthropogenic emissions in China according to C-REM outputs, while emissions in the rest of the world are kept unchanged. $PM_{2.5}$ concentrations reported here are calculated as the sum of sulfate, nitrate, ammonium, BC, OC, and dust concentrations following:

$$PM_{2.5} = 1.33 \times (SO_4 + NIT + NH_4) + BC + 1.8 \times (1.16 \times OCPI + OCPO) + 1.86 \times SALA + DST_1 + 0.38 \times DST_2$$

Where SO$_4$, NIT, and NH$_4$ represent sulfate-nitrate-ammonium aerosols, OCPO and OCPI represent hydrophobic and hydrophilic organic carbon, and SALA represents accumulation mode sea salt. DST1 and DST2 represent dust with size bins of 0.2-2.0 and 2.0-3.6 μm in diameter, respectively. DST2 is multiplied by 0.38 to reflect the mass fraction of PM$_{2.5}$ in DST2 assuming a log-normal size distribution. To convert dry aerosol concentrations from GEOS-Chem outputs to observed PM$_{2.5}$ which is often under a relative humidity of 35%, scaling factors of 1.33, 1.16, and 1.86 are used for sulfate-nitrate-ammonium, hydrophilic organic carbon, and sea salt aerosols, respectively. We use a conversion ratio from OC to organic matter of 1.8 based on measurements in Chinese cities (Xing et al., 2013). Anthropogenic PM$_{2.5}$ concentrations are sum of sulfate, nitrate, ammonium, BC, and OC. SOA is not included in the PM$_{2.5}$ calculation.

2.2.4 Health impacts and valuation

We calculated avoided premature deaths associated with reduction in total PM$_{2.5}$ atmospheric concentrations using the 2010 Global Burden of Disease (GBD) exposure-response relationships, covering the range of levels of global exposure to PM$_{2.5}$ (Burnett et al., 2014). We also used the Environmental Benefits Mapping and Analysis Program--Community Edition (BenMAP-CE; RIT International, 2015) to provide two additional estimates of avoided premature deaths (one using an exposure-response function estimated from Chinese data, and one using an exposure-response function based on U.S. data).

Following GBD, premature mortality due to five disease categories including acute lower respiratory illness (ALRI), chronic obstructive pulmonary disease (COPD), cerebrovascular disease (CEV), ischemic heart disease (IHD) and lung cancer (LC) attributed to ambient PM$_{2.5}$ in 2010 and 2030 was estimated from:

$$\text{Mort} = \sum_{i=1}^{5} pop_i \times y_{0i} \times (1 - 1/RR_i)$$

where i represents each of the five diseases, pop is the population of either children younger than 5 years (for ALRI) or adults older than 30 years (for IHD, CEV, COPD, and LC), y_0 is the baseline mortality rate for each disease, $(1-1/RR)$ is the attributable fraction of deaths due to PM$_{2.5}$, and RR is the relative risk which is calculated from the exposure response function based

on the Ambient Air Pollution Risk Model in the 2010 Global Burden of Disease Study (Institute for Health Metrics and Evaluation, 2013). The 2010 GBD exposure-response relationships, documented in Burnett et al. (2014), incorporate epidemiological studies of passive and active smokers to account for high $PM_{2.5}$ concentrations similar to those observed in China. COPD and CEV have different exposure response functions by age group with five-year intervals. We reported median mortality results using 1000 sets of RR values from Monte Carlo simulations.

Baseline mortality rates for each disease and each age group were obtained from the World Health Organization Statistics and Health Information System (World Health Organization, 2015). Gridded population in 2010 was accessed from the Columbia University Center for International Earth Science Information Network (CIESIN) with a spatial resolution of $0.5° \times 0.5°$ (CIESIN, 2005). Populations by country and by age group in 2010 and 2030 are taken from the United Nations World Population Prospects the 2015 revision (United Nations, 2015). We assume spatial distribution of population is unchanged in 2030.

We used BenMAP-CE to provide two additional estimates of avoided premature deaths. BenMAP-CE is an open-source program designed by the United States Environmental Protection Agency (U.S. EPA) and collaborators that calculates health impacts based on changes in air pollutant concentrations, baseline incidence of a health effect, population data, and a health effect coefficient that relates a change in air pollutant concentration with a change in incidence (RIT International, 2015). Vorhees et al (2014) provides a proof-of-concept methodology for using BenMAP-CE to perform health impact assessments on China, as well as documentation of the China data included in BenMAP-CE. We used baseline incidence and projected 2030 population data included in the China setup of BenMAP-CE. We used two all-cause mortality health effect coefficients from two epidemiological studies: Cao et al. (2011), which provides an exposure-response relationship based on Chinese data for adults greater than 40 years old, and Krewski et al. (2009), which provides an exposure-response relationship based on U.S. data for adults greater than 30 years old.

Mortality valuations are based on U.S. EPA's methodology and estimates for the Value of a Statistical Life (VSL), the suggested value of which is 7.75 million in 2007 U.S. dollars (EPA, 2014). Methods for calculating the VSL and a review of resulting estimates can be found in

Viscusi et al (2014). VSL for each Chinese province is based on the ratio of GDP per capita in 2030 relative to GDP per capita in 2007, similar to the procedure in Shindell et al. (2016):

$$VSL = VSL_{base} \times (pcGDP2007_{CHP} / pcGDP2007_{US} \times pcGDP2030_{CHP} / pcGDP2007_{CHP})^{0.4}$$

where $pcGDP_{CHP}$ and $pcGDP_{US}$ represent GDP per capita in 2007 (or 2030) for each Chinese province and the U.S., respectively. Income elasticity of the VSL with respect to per capita GDP is set to be 0.4 (Hammitt and Robinson, 2011).

For comparison, we also calculate co-benefits using a VSL based on Chinese data (Wang and He, 2010), which corresponds to a year 2007 VSL of U.S. $165,600 with an income elasticity of 0.42.

2.3 Results

At national level, the 4% Policy scenario leads to a 24% reduction in CO_2 emissions in 2030, relative to the No Policy case. The CO_2 price required to achieve these reductions rises to $72/ton in 2030 ($CO_2$ prices are reported in 2007 U.S. dollars). Most of the CO_2 reduction in 2030 is a result of a 20% energy intensity reduction (relative to the No Policy scenario in 2030), reflecting the combined effect of higher energy efficiency and sectoral composition change. Coal is substantially affected. Under the 4% Policy, coal represents 53% of total energy use in 2030, down from 69% in 2010, while substitution towards clean energy contributes only modestly (see Figure 2.3 (a)). Figures 2.3 (b)-(d) show sectoral reductions in energy use and emissions under the 4% Policy. The energy-intensive and manufacturing sector, which includes iron and steel, non-ferrous metals, non-metallic materials, and chemicals, experiences the largest reduction in energy use and emissions of CO_2 and air pollutants. The electricity sector, which consumes primarily coal, experiences the second largest reduction. Oil use in transportation is less affected: it has a lower CO_2 emissions factor compared to coal, and has few cost-effective substitutes. As policy stringency increases, the CO_2 price increases from $26/ton with a 3% Policy to $132/ton with a 5% Policy in 2030. CO_2 emissions in the 4% Policy case are projected to peak in 2025 at 11.5 bt, and are estimated to peak in 2020 at 10.6 bt in the 5% Policy case. CO_2 emissions trajectories are shown for all cases in Figure 2.4 (a).
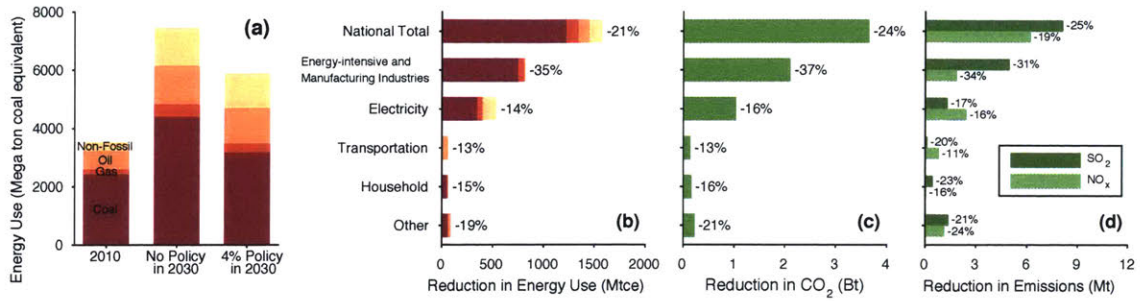
Figure 2.3. Changes in energy use and emissions in the 4% Policy scenario compared to the No Policy scenario in 2030. a,b, Changes in energy use at the national (a) and sectoral (b) levels. Mtce, million tons of coal equivalent. c,d, Sectoral reductions in CO_2 (c) and SO_2 and NO_x (d) emissions (with percentage changes to the right of each bar) in the 4% Policy scenario compared to the No Policy scenario in 2030.

Regionally, simulated changes in consumption, energy use, and CO_2 emissions under the 4% Policy compared to the No Policy scenario vary widely across China's provinces (Figure A.1). Substantial CO_2 emissions reductions in both relative and absolute terms occur in Shanxi, Guizhou, and Inner Mongolia (by 51%, 43%, and 35%, respectively), largely in the mining and energy-intensive manufacturing sectors, reflecting abundant low-cost opportunities to improve coal use efficiency in provinces with a large share of energy-intensive industry and high energy intensity. Economic impacts in terms of changes in consumption are also larger in these provinces because their coal production accounts for a large share of provincial GDP. Importantly, the provincial distribution of policy costs depends on the initial allocation of emissions allowances (D. Zhang et al., 2016). In our simulation, CO_2 emissions allowances are initially distributed according to 2010 emissions and increased over time in proportion to provincial GDP. Projected co-benefits could provide a basis for adjusting this allocation across provinces to limit uneven impacts.

National-level impacts of climate policy on pollutant reductions vary widely. We focus on sulfur dioxide (SO_2), nitrogen oxides (NO_x), and ammonia (NH_3), which combine in the atmosphere to form inorganic $PM_{2.5}$, as well as black carbon (BC) and primary organic carbon (OC) (see Figures 2.4 (b)-(f)). Climate policies lead to the largest reductions in SO_2 and NO_x because these emissions are closely associated with coal combustion, the energy type most impacted by policy. Under the 4% Policy, we find a 25% reduction in SO_2 and a 19% reduction

31

in NO_x in 2030 relative to the No Policy scenario. Climate policies have a limited effect on NH_3, because >80% of NH_3 is emitted from the agricultural sector.
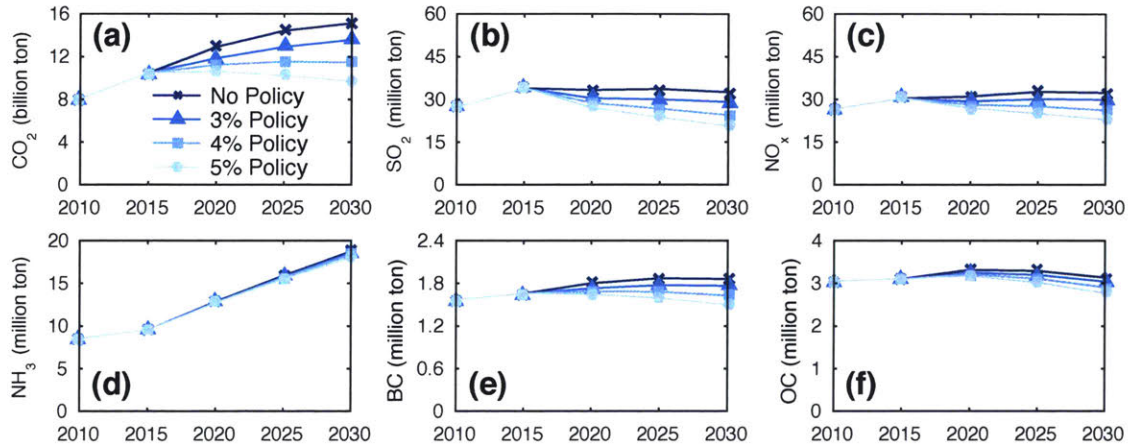
Figure 2.4. Impacts of changing policy stringency on emissions of CO_2 and air pollutants. a–f, Simulated CO_2 (a) and pollutant emissions (b–f) under the No Policy scenario and Policy scenarios targeting annual CO_2 intensity reductions ranging from 3% to 5%. The legend in (a) applies to all panels.

The No Policy scenario in 2030 has a national population-weighted annual average $PM_{2.5}$ concentration of 70.1 $\mu g/m^3$. This $PM_{2.5}$ concentration falls by 4.7% under the 3% Policy, 12% under the 4% Policy, and 19% under the 5% Policy (these levels represent an increase of 21%, 12%, and 3.5% relative to 2010, respectively) (see Figure 2.5). Modest changes in national population-weighted $PM_{2.5}$ mask large variation in provincial impacts. Comparing Figures 2.5 (a) and (b), air quality in central China degrades more than in western China, where projected economic growth rates, reflected in government plans, are higher. Climate policies therefore deliver larger air quality benefits in this region (Figures 2.5 (c)-(e)). Of Central China provinces, north and southwestern China, which include several coal consumption centers, experience relatively greater air quality improvements. In contrast, the most populated eastern regions experience less improvement. Larger shares of light industry and services in these economies limit CO_2 reduction opportunities from more energy-intensive sectors. These economies also have higher pre-existing energy efficiency, making incremental CO_2 reductions relatively costly. Under the 4% Policy, population-weighted $PM_{2.5}$ decreases by 14-15% in urban Beijing, Tianjin, and Hebei, and decreases 10-11% in coastal Jiangsu, Zhejiang, Fujian, and Guangdong, relative to 2030 levels in the No Policy scenario (Figures A.1).
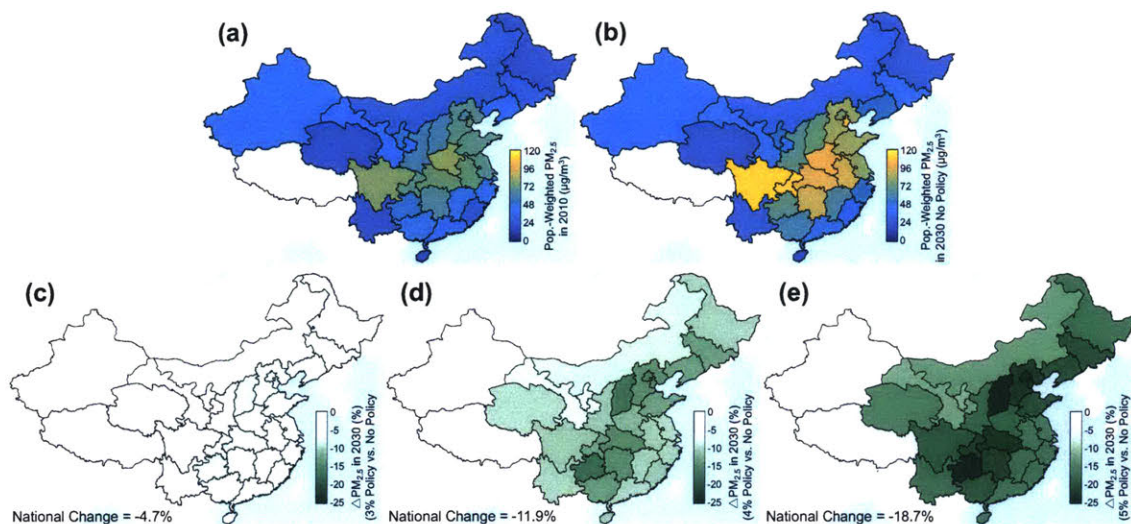
Figure 2.5. Spatial distribution of population-weighted PM$_{2.5}$. a, b, The annual average of population-weighted PM$_{2.5}$ concentrations in 2010 (a) and under the No Policy scenario in 2030 (b). c–e, Difference in 2030 population-weighted PM$_{2.5}$ concentrations between the Policy scenarios (3%, 4% and 5%) and the No Policy scenario.

At national level in 2030, total premature mortalities in the No Policy scenario are >2.3 million, and projected PM$_{2.5}$ reductions result in 36,000, 94,000, and 160,000 avoided premature mortalities in the 3%, 4%, and 5% Policy scenarios, respectively, using exposure-response relationships from the Global Burden of Disease study (Burnett et al., 2014). Estimated avoided premature deaths in 2030 under the 4% Policy scenario are more than an order of magnitude higher than those estimated for the U.S. Clean Power Plan in 2030 (Driscoll et al., 2015). Avoided mortalities using alternative exposure-response relationships are provided in Table A.3. For nearly all provinces, the BenMAP-CE results bound the GBD estimate. In five provinces (Guangdong, Fujian, Shanghai, Hainan, Fujian, and Xinjiang), the GBD estimate is higher than both BenMAP-CE results, and for Shaanxi it is lower, but all are still within the same order of magnitude. Health co-benefits in the 4% Policy scenario are 3.7 times larger than policy costs if international estimates are used for health valuation, while co-benefits only offset 26% of policy costs using recent Chinese estimates. For comparison, we also calculate co-benefits using a VSL based on Chinese data (Wang and He, 2010). Calculated health benefits using this VSL are U.S. $12.1 billion, $32.6 billion, and $55.6 billion in the 3%, 4% and 5% policy cases, respectively. Monetized values of health co-benefits (before considering policy

cost) vary widely across provinces, from $1.6 billion in Ningxia to $53.7 billion in Guangdong in the 4% Policy scenario.

2.4 Discussion

The set of relationships affecting health co-benefits from climate policy in each province, denoted by subscript i, is captured by the relationship in equation (1). Each ratio in equation (1) is governed by non-linear, interacting processes. The monetary value of health co-benefits changes (in percentage terms) ΔHCB_i due to policy is affected by associated changes in mortality (ΔM_i), relationships between mortality and $PM_{2.5}$ changes ($\Delta PM_{2.5,i}$, the concentration-response relationship), $PM_{2.5}$ reduction delivered as a result of CO_2 emissions reduction ($\Delta CO_{2,i}$), and CO_2 emissions reduction associated with changes in energy use (ΔE_i). At national level, these relationships are illustrated in Figure 2.6 (a) for varying policy stringency, and in Figure 2.6 (c) by province for the 4% Policy scenario. The relationship between economic cost and avoided health damages by province is shown in Figure 2.6 (b).

$$\Delta HCB_i = \frac{\Delta HCB_i}{\Delta M_i} \times \frac{\Delta M_i}{\Delta PM_{2.5,i}} \times \frac{\Delta PM_{2.5,i}}{\Delta CO_{2,i}} \times \frac{\Delta CO_{2,i}}{\Delta E_i} \times \Delta E_i \quad (1)$$

$$\frac{\Delta PM_{2.5,i}}{\Delta CO_{2,i}} = \frac{\Delta PM_{2.5,i}}{\Delta precursors_i} \times \frac{\Delta precursors_i}{\Delta CO_{2,i}} \quad (2)$$

As shown in Figure 2.6 (a), the relative reduction of population-weighted $PM_{2.5}$ at national level in each scenario is less than proportional to the associated CO_2 reduction. Equation (2) captures a critical step that explains this. $\Delta PM_{2.5,i}$ / $\Delta CO_{2,i}$ depends on relative changes in the inorganic precursors that combine to form $PM_{2.5}$: SO_2, NO_x, and NH_3. Complexes of ammonium nitrate and ammonium sulfate are important components of $PM_{2.5}$. Climate policy reduces SO_2 proportionally more than NH_3, because the former is co-emitted with CO_2 from power plants and industrial facilities, while the latter is primarily emitted from agricultural sources. NO_x is reduced proportionally less than SO_2 because NO_x is emitted from vehicles as well as power plants, and vehicles are less impacted by the policy. Thus, as policy stringency increases, SO_2 falls most, NO_x falls moderately, and NH_3 falls least, with this ratio varying across provinces. Although the relative sulfate reduction is nearly proportional to CO_2 reduction, the relative nitrate reduction is significantly lower. Co-benefits from the reduction of sulfate-nitrate-

ammonium aerosols account for 87% of total $PM_{2.5}$ co-benefits. The contribution from BC and primary OC is significantly lower because their emissions are mostly from biomass burning, which is not directly affected by a climate policy targeting CO_2. Secondary organic aerosols (SOA) are not included in this analysis since their main precursors (volatile organic compounds, VOCs) are only slightly targeted by the policy (2-10%), and SOA only accounts for about 5% of Chinese annual mean $PM_{2.5}$ in GEOS-Chem (see e.g. Fu et al., 2012). Further, GEOS-Chem resolves major Chinese urban centers in 6-8 grid boxes, which may dilute localized poor air quality, affecting projected health effects. For the U.S., however, Thompson et al. (2014) found calculated benefits were robust to resolution selected.

To illustrate the influence of chemical interactions, and since NH_3 projections are uncertain, we conduct GEOS-Chem simulations with NH_3 emissions constant at 2010 levels, around 46% of that in the No Policy scenario in 2030. Results show limiting the NH_3 increase results in a further 12.3% reduction in population-weighted $PM_{2.5}$ under the 4% Policy scenario. Co-benefits in $PM_{2.5}$ concentrations under the 4% Policy fall from 12% to 9.7% if NH_3 emissions are kept at 2010 levels because of reduced co-benefits from nitrate. This exercise illustrates the importance of accounting for and controlling NH_3 as a complementary and even synergistic measure alongside climate policy, as suggested by earlier studies (Wang et al., 2011; Wang et al., 2013).

At provincial level, the relationship between CO_2 and anthropogenic $PM_{2.5}$ change is shown in Figure 2.6 (c). Although SO_2 and NO_x emissions are reduced nearly in proportion to CO_2 emissions, the reduction in anthropogenic $PM_{2.5}$ is smaller, mainly because of the relatively small change in NH_3 emissions and the limited availability of SO_2 and NO_x oxidants. In addition, we find variation in this relationship across provinces, which reflects regional variations in the composition of the energy system and abatement costs, pollutants and resulting chemistry, and transport of air pollutants from neighboring provinces. For example, Beijing, the national capital and a populous urban center with limited coal-intensive industry, reduces CO_2 emissions and anthropogenic $PM_{2.5}$ by 19% and 18% respectively under the 4% Policy scenario. This relatively large reduction in anthropogenic $PM_{2.5}$ follows from the fact that the least-cost CO_2 abatement opportunities pursued under the policy also reduce SO_2 emissions from its few remaining sources. As a result, Beijing has relatively large net benefits per capita (Figure 2.6

(b)). In contrast, the reduction of anthropogenic $PM_{2.5}$ in Shanxi is only 23% despite reducing CO_2 emissions by 51%. This non-linearity is largely due to local atmospheric chemistry: a limited decrease in nitrate concentration in response to the 45% decline of NO_x emissions. Considering total $PM_{2.5}$, including contributions from non-anthropogenic sources such as dust, relative changes correlate even less with CO_2 reductions (see Figure A.3 for provincial results comparing anthropogenic and total $PM_{2.5}$).

At the national level, avoided mortality rises as policy stringency increases, as shown in Figure 2.6 (a), but its relative increase is lower than for $PM_{2.5}$. Nevertheless, avoided mortality translates into net health co-benefits that rise faster than policy costs. Net co-benefits based on an international value of statistical life (VSL) approach are projected to be U.S. $138.4 billion in the 3% Policy scenario (U.S. $173.1 billion in health co-benefits minus U.S. $34.7 billion in costs), U.S. $339.6 billion in the 4% Policy scenario (U.S. $464.5 billion in health co-benefits minus U.S. $125.0 billion in costs), and U.S. $534.8 billion in the 5% Policy scenario (U.S. $790.7 billion minus U.S. $255.9 billion). Coal represents a large initial share of the energy mix, and remains the marginal fuel reduced by climate policy over the range of policy stringency considered. Reducing coal use, which continues with increasing policy stringency, brings large reductions in co-emitted pollutants.
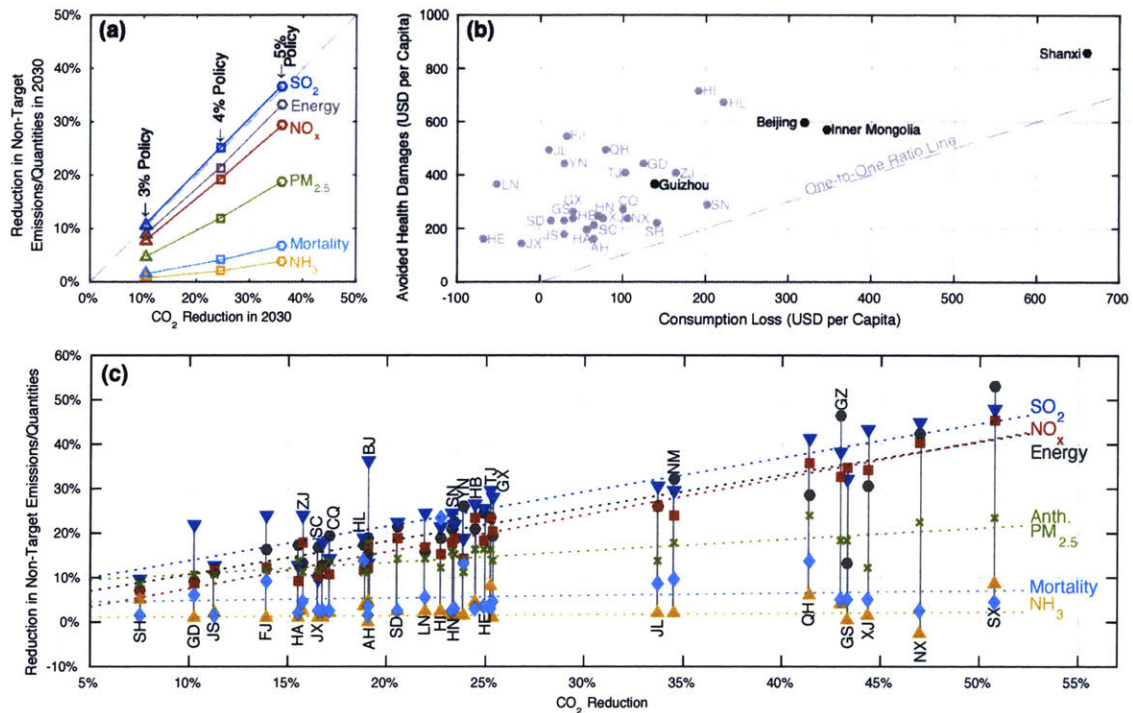
Figure 2.6. Air quality co-benefits of climate policy. a, Reduction in non-target pollutants/quantities under different national-level policy stringencies, b, Provincial distribution of policy costs and avoided health damages per capita in 2030 under the 4% Policy (Province name abbreviations are listed in Table A.1). c, Provincial distribution of reductions in non-target pollutants/quantities in 2030 under the 4% Policy (dotted lines denote linear trends for each pollutant/quantity). Detailed provincial results are presented in Figs. A.3 and A.4.

Our framework could be readily extended to study the impact of other policies and technologies on a wide range of sustainability outcomes. For instance, it could be extended to consider the air quality co-benefits of other climate policies (e.g. renewable energy subsidies) or to study the climate co-benefits of air quality policies, which would require augmenting the model with the costs of air pollution control technologies. Our framework could further be extended to capture other unintended consequences of policy, such as impacts on agriculture and water supplies, allowing for more holistic analysis of sustainability impacts.

2.5 Implications for Climate and Sustainability Policy

Air quality improvement is a valuable co-benefit of carbon pricing that increases with policy stringency in China. Even without considering the social cost of carbon (Tol et al., 2011), a measure of direct benefits of climate policy per ton CO_2 reduced, health co-benefits can

outweigh policy costs to households. This is relevant for other developing nations, especially those that rely on coal with limited end-of-pipe pollution control. As China has formally announced plans to introduce a national emissions trading system, our results suggest that such a system covering many energy-intensive sectors could have large aggregate benefits, providing a powerful incentive for adoption, but uneven local impacts. Our results show that even a modest CO_2 price would yield substantial net health co-benefits, while tightening policy over the range considered here would increase them. We also note that the CO_2 price itself will not achieve Chinese ambient air quality standards (China MEP, 2012) with an annual average limit of 35 $\mu g/m^3$ in 2030; further end-of-pipe control and reduction of pollution from non-combustion sources, e.g. NH_3, will be needed. Our framework further reveals the difficulties associated with balancing coverage of a large area to maximize cost-effective abatement against the recognition that concomitant air quality improvements will not always occur where potential health benefits are greatest. Therefore, policy makers should consider how carbon policy and air quality control policy interact when formulating new proposals.

Chapter 3 Co-benefits of China's climate policy for air quality and human health in China and transboundary regions

Abstract

Climate policies targeting CO_2 emissions from fossil fuels can simultaneously reduce emissions of air pollutants and their precursors, thus mitigating air pollution and associated health impacts. Previous work has examined co-benefits of climate policy from reducing $PM_{2.5}$ in rapidly-developing countries such as China, but have not examined co-benefits from ozone and its transboundary impact for both $PM_{2.5}$ and ozone. Here, we compare the air quality and health co-benefits of China's climate policy on both $PM_{2.5}$ and ozone in China to those in three downwind and populous countries (South Korea, Japan and the United States) using a coupled modeling framework. In a policy scenario consistent with China's pledge to peak CO_2 emissions in 2030, health co-benefits from ozone reductions are 54,300 (95% confidence interval: 37,100–71,000) in China, nearly 60% of those from $PM_{2.5}$. Total avoided premature deaths in South Korea, Japan, and the US are 1,200 (900—1,600), 3,500 (2,800—4,300), and 1,900 (1,400—2,500), respectively. Total avoided deaths in South Korea and Japan are dominated by reductions in $PM_{2.5}$-related mortality, but ozone plays a more important role in the US. Similar to co-benefits for $PM_{2.5}$ in China, co-benefits for ozone and for both pollutants in those downwind countries also rise with increasing policy stringency.

3.1 Introduction

Exposure to air pollution, including $PM_{2.5}$ and ozone can cause cardiovascular and respiratory diseases, and is estimated to be responsible for 3.3 million premature deaths in 2010 worldwide (Lelieveld et al., 2015). Combustion of fossil fuels, particularly coal, is a major source of both primary $PM_{2.5}$ and precursors that lead to formation of $PM_{2.5}$ and ozone, such as sulfur dioxide (SO_2) and nitrogen oxides (NO_x). China's dense population and high coal share in energy

consumption make it one of the world's most polluted countries (van Donkelaar et al., 2016; Ma et al., 2017). Air pollutants and their precursors from China can also travel long distances, and studies have estimated that Asian anthropogenic emissions contributed to ~1 ppb of surface ozone averaged in the US for 2001–2005 with higher influence over the western part and in spring (Brown-Steiner and Hess, 2011; Zhang et al., 2008), and ~0.2 $\mu g/m^3$ of surface $PM_{2.5}$ in the US in 2000 (Leibensperger et al., 2011). Anenberg et al. (2009) found that about 27% of the reduced premature deaths that resulted from a 20% decrease in anthropogenic precursors of ozone in East Asia occur outside of this region, and this figure is only 2% for $PM_{2.5}$ due to its shorter lifetime in the atmosphere (Anenberg et al., 2014). However, the absolute reduction in deaths due to changes in $PM_{2.5}$ is greater than that of ozone because of the larger effect of $PM_{2.5}$ on mortality (Anenberg et al., 2014). Q. Zhang et al. (2017) estimated that $PM_{2.5}$ pollution produced in China in 2007 was responsible for 64,800 premature deaths in regions other than China.

Climate policies that limit fossil fuel combustion can also reduce co-emitted air pollutants, thus having co-benefits for air quality and human health. This effect has been quantified extensively in the literature on both global and regional scales (e.g. West et al., 2013; Thompson et al., 2014). Under the 2015 Paris Agreement, China has committed to achieve a peak in national CO_2 emissions and to increase its non-fossil share of primary energy to 20% by 2030. A global study (West et al., 2013) quantified the co-benefits of climate policy under the representative concentration pathways for $PM_{2.5}$ and ozone concentrations, and their associated premature deaths in 2030, 2050 and 2100, but did not take into account China's recent climate policy, nor separate the influence from Chinese anthropogenic emissions on transboundary regions. Some more recent studies have considered China's up-to-date climate policy and evaluated its air quality and health co-benefits. Peng et al. (2018) found that electrification of transport and residential sectors with a half-decarbonized power supply (50% coal) can prevent 55,000-69,000 deaths nationally in 2030. Li et al. (2018) found that a climate policy scenario in which CO_2 emissions peaked in 2030 would avoid 94,000 premature mortalities in 2030. Both studies only quantified co-benefits from $PM_{2.5}$ reduction, since $PM_{2.5}$ is found to have a much larger contribution to premature deaths than ozone (Lelieveld et al., 2015). However, a recent study estimated a higher positive association between ozone concentration and respiratory mortality (Turner et al., 2016), which would lead to larger co-benefits from ozone reductions. In addition,

ozone has a longer lifetime in the atmosphere than $PM_{2.5}$, making it relatively more important in transboundary regions.

In this study, we quantify the co-benefits of China's climate policy under three different stringencies on both $PM_{2.5}$ and ozone concentrations and their associated health impact in China and three downwind and populous countries including South Korea, Japan, and the US. We use a modeling framework developed by Li et al. (2018) which links an energy-economic model with sub-national detail for China (the China Regional Energy Model, or C-REM) and a global atmospheric chemistry model (GEOS-Chem).

3.2 Methods

Using C-REM, we simulate a No Policy scenario and three policy scenarios that target CO_2 intensity reductions of 3%, 4%, and 5% per year between 2015 and 2030 (denoted as 3% Policy, 4% Policy, and 5% Policy scenarios). Gridded emissions of air pollutants in 2030 for each scenario are derived by scaling gridded emissions in 2015 based on projected provincial-level emissions from C-REM, and then used as input to GEOS-Chem to simulate $PM_{2.5}$ and ozone concentrations. Air quality co-benefits of climate policy are defined as the reduction in surface concentrations of $PM_{2.5}$ and ozone between the No Policy scenario and each of the three policy scenarios in 2030. Associated avoided $PM_{2.5}$- and ozone-related premature deaths due to climate policy are calculated using the concentration-response functions (CRFs) in Burnett et al. (2014) and Turner et al. (2016), respectively.

C-REM is a global general equilibrium model that resolves China's economy and energy system at the provincial level, including production, consumption, interprovincial and international trade, energy use, and emissions of CO_2 and air pollutants. The model has a base year of 2007 and is solved at five-year intervals through 2030. It is calibrated to historical data in 2010 and 2015. CO_2 intensity reduction targets under the three policy scenarios are achieved by establishing different CO_2 prices in C-REM that lead to deployment of least-cost CO_2 reduction strategies. In C-REM, emissions of air pollutants by province and by sector are calculated from projected energy use (for combustion sources) or economic activity (for non-combustion sources), multiplied by corresponding emissions factors. In this study, we consider all the major precursors of $PM_{2.5}$ and ozone — SO_2, NO_x, ammonia (NH_3), black carbon (BC),

41

organic carbon (OC), carbon monoxide (CO), and non-methane volatile organic compounds (NMVOCs). Emissions factors by province, by sector and by energy type for each pollutant in 2007 are derived from the Regional Emission Inventory in Asia (REAS, Kurokawa et al., 2013). Emissions factors in 2010 and 2015 are calibrated based on national total emissions reported in the Multi-resolution Emission Inventory for China (MEIC: http://www.meicmodel.org). In order to account for future improvement in emission control measures, we assume emission factors continue to decrease exponentially after 2015 by adopting the methodology from Webster et al. (2008), where the exponential decay factors of each species are determined based on historical emission trends in 15 developed countries. Further details on C-REM, matching of sectors and energy type between C-REM and REAS, calibration in 2010 and 2015 with the MEIC inventory, and exponential decay in emissions factors after 2015 are documented in Li et al. (2018).

Provincial-level emission outputs from C-REM in 2007, 2010, 2015 and the four scenarios in 2030 are used to scale gridded REAS emissions in 2007 to estimate gridded emissions in later years, which are then used in the chemical transport model GEOS-Chem to simulate $PM_{2.5}$ and ozone concentrations. We use version 9-01-03 with a horizontal resolution of $2° \times 2.5°$ globally and $0.5° \times 0.667°$ in East Asia. Each simulation is one-year long with a six-month spin-up period. Further information on the simulation configuration can be found in Li et al. (2018). $PM_{2.5}$ concentrations reported here are calculated by summing over sulfate, nitrate, ammonium, BC, OC, and dust concentrations following:

$$PM_{2.5} = 1.33 \times (SO_4 + NIT + NH_4) + BC + 1.8 \times (1.16 \times OCPI + OCPO) + 1.86 \times SALA + DST_1 + 0.38 \times DST_2$$

Where SO4, NIT, and NH_4 represent sulfate, nitrate, and ammonium aerosols, respectively, OCPI and OCPO represent hydrophilic and hydrophobic organic carbon, and SALA represent accumulation mode sea salt. DST1 and DST2 represent dust with size bins of 0.2–2.0 and 2.0–3.6 μm in diameter, respectively. Scaling factors of 1.33, 1.16, and 1.86 are used for SO4-NIT-NH4, OCPI, and SALC respectively to convert dry aerosol concentrations from GEOS-Chem outputs to measured $PM_{2.5}$ which is often under a relative humidity of 35% (Chow and Watson, 1998). We convert organic carbon to organic matter using a ratio of 1.8 based on measurements in Chinese cities (Xing et al., 2013). DST2 is multiplied by 0.38 to reflect the mass fraction of $PM_{2.5}$ in this size bin, assuming a log-normal size distribution.

Using measurements of sulfate, nitrate, ammonium, BC, OC, and total $PM_{2.5}$ taken between 2005 and 2010, we find that GEOS-Chem can generally reproduce the observed spatial distribution of $PM_{2.5}$ and its species with correlation coefficients (R) greater than 0.6 (detailed comparisons are shown in Li et al., 2018). We also compare our simulated monthly ozone concentrations in 2007 with measured monthly values averaged a few years before 2007 at seven observation sites in East China (Li et al., 2007; Lin et al., 2008; Wang et al., 2009; Wang et al., 2011; Yang et al., 2008). Details of the observation sites are listed in Table 3.1, and comparison for each site is shown in Figure 3.1. GEOS-Chem captures the seasonal variation in ozone concentrations indicated by correlation coefficients (R) ranging from 0.62 to 0.91, and annual-average model biases are within 5 ppb (with the exception of the Miyun site).

Table 3.1. List of ozone measurements used in this study.

Site	Measurement period	Longitude (°)	Latitude (°)	Height (m)	Reference
Lin'an	Nov.2003-Nov.2004	119.7	30.3	139	Yang et al. (2008)
Hong Kong	1994-2007	114.3	22.2	60	Wang et al. (2009)
Miyun	2006	116.8	40.5	152	Wang et al. (2011)
Shangdianzi	2004-2006	117.1	40.7	294	Lin et al. (2008)
Mount Tai	2004-2005	117.1	36.3	1533	Li et al. (2007)
Mount Hua	2004-2005	110.1	34.5	2064	Li et al. (2007)
Huangshan	2004-2005	118.2	30.1	1836	Li et al. (2007)
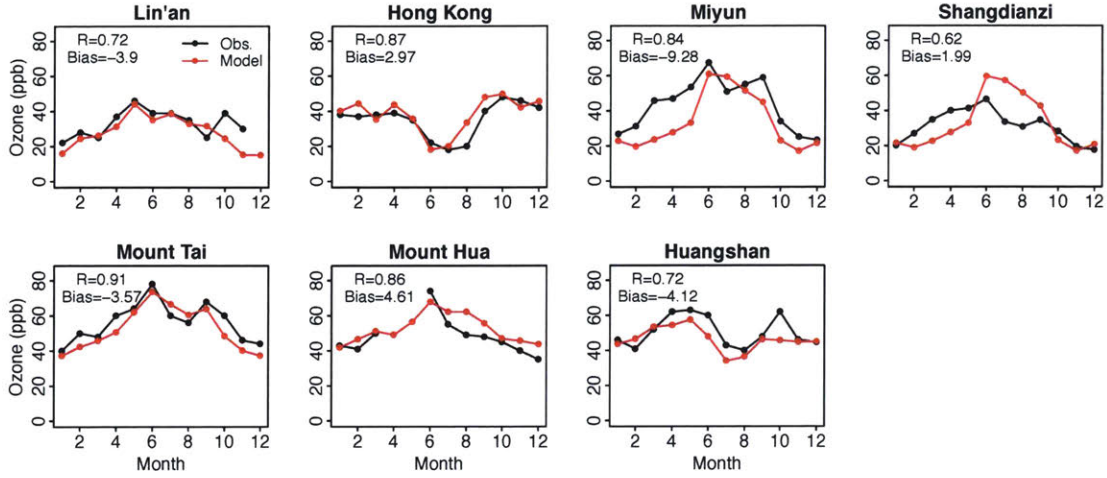
Figure 3.1. Comparisons of monthly-mean ozone concentrations from observational sites listed in Table S1 and model simulation in 2007. Correlation coefficient (R) and averaged bias between model and observation at each site are shown in the top left of each subplot.

Premature deaths attributed to $PM_{2.5}$ from acute lower respiratory illness (ALRI), ischemic heart disease (IHD), cerebrovascular disease (CEV), chronic obstructive pulmonary disease (COPD), and lung cancer (LC) in 2030 in each grid cell are estimated from:

$$\text{Mort} = \sum_{i=1}^{5} pop_i \times y_{0i} \times (1 - 1/RR_i)$$

Where i represents each of the five diseases, pop is the population of either children younger than 5 years (for ALRI) or adults older than 30 years (for IHD, CEV, COPD, and LC), y_0 is the baseline incidence rate of a certain disease, $(1-1/RR)$ is the attributable fraction of deaths due to $PM_{2.5}$, and RR is the relative risk defined as the ratio of incidence rates between exposed and unexposed populations. Here RR is calculated from the CRF in the 2010 GBD study (Burnett et al. 2016), which incorporates epidemiological studies of passive and active smoking and indoor air pollution to account for high $PM_{2.5}$ concentrations:

$$RR = 1 + \alpha \left\{ 1 - exp \left[-\gamma (c - c_{cf})^{\delta} \right] \right\}$$

where c is the simulated $PM_{2.5}$ concentration in $\mu g/m^3$, c_{cf} is the counterfactual concentration below which there is no additional risk, α, γ, and δ are coefficients that determine the shape of CRF. We use the distribution of CRFs provided by Burnett et al. (2016) for each disease,

44

specifically, 1000 sets of c_{cf}, α, γ, and δ from Monte Carlo simulations for ALRI, COPD and LC, and age-specific CRFs (1000 sets of parameters) in every five-year age interval for IHD and CEV. Avoided deaths due to climate policy from $PM_{2.5}$ are the difference in premature deaths between the No Policy scenario and each of the policy scenarios. The median values and 95% confidence intervals (CIs) of total avoided deaths for all five diseases in each country reported here are summed from 100,000 bootstrap simulations.

Avoided premature deaths due to climate policy attributable to ozone are estimated from:

$$\Delta Mort = pop \times y_0 \times (1 - 1/RR)$$

We use a log-linear CRF between change in ozone concentration and RR:

$$RR = exp(-\beta \Delta c)$$

where *pop* is the population of adults older than 30 years, Δc is the change in ozone concentration between No Policy scenario and each of the policy scenarios in ppb, and β is the CRF slope calculated from a recent estimate of RR per 10 ppb increase in annual mean of maximum daily 8-hour average (MDA8) ozone of 1.12 (95% CI: 1.08-1.16) for respiratory diseases and 1.03 (95% CI: 1.01-1.05) for circulatory diseases (Turner et al., 2016). Avoided deaths of each disease are sampled 100,000 times from the normal distribution of RR, and the median values and 95% CIs of total avoided deaths are summed from 100,000 bootstrap simulations. We use daily 10am–6pm average ozone concentration as a proxy for MDA8 ozone concentration. For comparison, we also calculated avoided deaths using an older CRF with RR per 10 ppb increase in the maximum 6-month average of 1-h daily ozone extreme of 1.040 (95% CI: 1.013–1.067) for respiratory diseases (Jerrett et al., 2009). We increase the Δc of MDA8 ozone averaged from April to September by 10% to represent the maximum 6-month average of 1-h daily ozone extreme following Shen et al. (2017).

Baseline mortality rates for each country and each disease are obtained from the World Health Organization Mortality Database (World Health Organization, 2015). We use mortality rates of the most recent available year in the dataset, which is the year 2000 for China, 2013 for South Korea and Japan, and 2007 for the US. Country-specific baseline mortality rates for $PM_{2.5}$- and ozone-related diseases are listed in Table 3.2. We assume mortality rates are unchanged in 2030.

Gridded population in 2030 is derived by scaling gridded population data in 2010 from the NASA Socioeconomic Data and Applications Center (NASA SEDAC, 2005), based on population projections by country and by age group in 2030 from the United Nations World Population Prospects 2015 revision under a median fertility scenario (United Nations, 2015) assuming that the spatial distribution of population in each country in 2030 is the same as that in 2010.

Table 3.2. Baseline mortality rates in deaths per 1000 people (aged <5 years for ALRL and >30 years for other diseases).

	Year	$PM_{2.5}$ related					Ozone related	
		IHD	CEV	COPD	LC	ALRI	Circulatory	Respiratory
China	2000	1.02	2.34	1.68	0.62	0.42	4.52	2.00
South Korea	2013	0.41	0.77	0.21	0.52	0.01	2.05	0.68
Japan	2013	0.82	1.30	0.21	0.80	0.02	3.95	2.24
US	2007	2.30	0.77	0.72	0.90	0.02	4.97	1.28

3.3 Results

3.3.1 Co-benefits under the 4% Policy scenario

Figure 3.2 shows reductions of precursor emissions under the 4% Policy scenario compared to the No Policy scenario in 2030. Climate policy limits fossil fuel use in proportion to carbon content, therefore air pollutants that mostly come from fossil fuel such as SO_2, NO_x, and CO emissions are reduced by 17-25%. Their reductions are much greater than NH_3 and NMVOCs (2-6%) which are mainly from agriculture and industrial processes, respectively. Emission reduction also differs by province. Larger reductions of SO_2 and NO_x emissions are found in Guizhou, Shanxi, and Shandong provinces since they have a larger share of energy-intensive industries and abundant low-cost opportunities to improve coal use efficiency. NH_3 emissions decline more in Hunan and Hubei provinces.
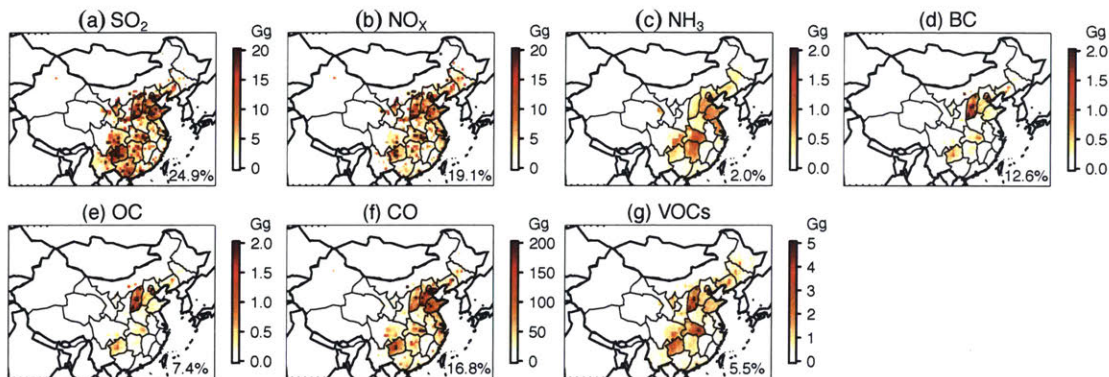
Figure 3.2. Reductions in precursor emissions under the 4% Policy scenario compared to the No Policy scenario in 2030 in gigagram per grid cell: (a) SO_2, (b) NO_x, (c) NH_3, (d) BC, (e) OC, (f) CO, and (g) NMVOCs. Numbers in the bottom right corner represent the percentage reductions in national total emissions.

Figure 3.3a and 3.3b shows the reductions in simulated annual-mean surface concentrations of $PM_{2.5}$ under the 4% Policy scenario compared to the No Policy scenario in East Asia and the US in 2030. Larger $PM_{2.5}$ co-benefits are found in North China, Central China, Sichuan, and Guizhou provinces, due to a larger reduction in both sulfate and nitrate aerosols in these regions (Figure 3.4a and 3.4c). The population-weighted concentration of $PM_{2.5}$ in China is reduced by 8.3 $\mu g/m^3$ from 69.9 $\mu g/m^3$ in the No Policy scenario to 61.6 $\mu g/m^3$ in the 4% Policy scenario, as discussed further in Li et al. (2018). Inorganic aerosols (sulfate, nitrate, and ammonium) account for 87% of the total co-benefits with sulfate contributing 39% and nitrate contributing 26% (Table 1). Reduction in $PM_{2.5}$ is diluted downwind of China. As a result, population-weighted $PM_{2.5}$ in South Korea, Japan, and the US are reduced by 1.7, 0.5, and 0.04 $\mu g/m^3$, respectively, relative to No Policy. These reductions are one to two orders of magnitude smaller than that in China. Reductions in downwind countries are also primarily due to sulfate. The contribution from sulfate increases from 53% in South Korea to 70% in the US (Table 3.2 and Figure 3.4). The dilution effect of sulfate reduction is weaker than that of nitrate, because transported SO_2 continues to oxidize to sulfate along the transport pathway (Figure 3.5). Sulfate reduction is fairly uniform over the US, whereas nitrate reduction occurs in the Midwest where local NO_x emissions are higher (Figure 3.4).

Table 3.3. Projected air quality co-benefits for the 4% Policy scenario in China and three downwind countries in 2030. Values are population-weighted averages.

	PM$_{2.5}$ (μg/m^3)	Sulfate (μg/m^3)	Nitrate (μg/m^3)	Ammonium (μg/m^3)	BC (μg/m^3)	OC (μg/m^3)	MDA8 ozone (ppb)
China	8.33	3.21	2.20	1.82	0.37	0.74	1.57
South Korea	1.66	0.87	0.22	0.38	0.06	0.13	0.55
Japan	0.51	0.32	0.02	0.12	0.02	0.04	0.46
US	0.04	0.03	0.001	0.01	0.001	0.001	0.20
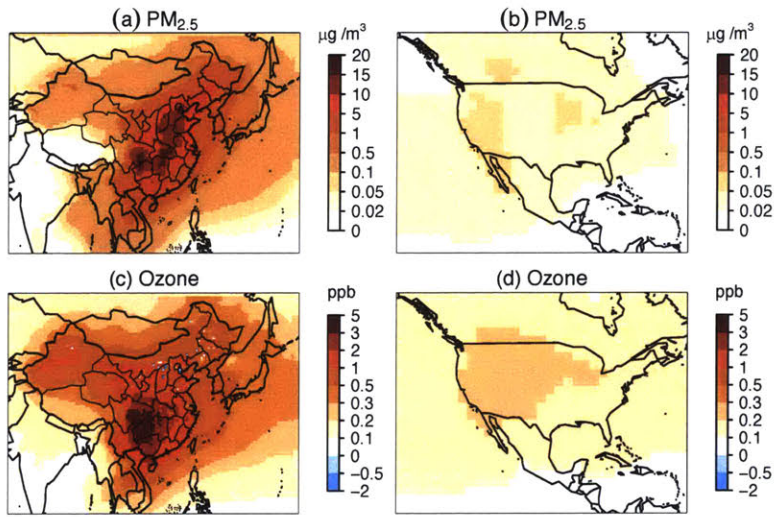
Figure 3.3. Reductions in simulated annual-mean surface concentrations of PM$_{2.5}$ (a, b) and MDA8 ozone (c, d) under the 4% Policy scenario compared to the No Policy scenario in East Asia and the US in 2030.
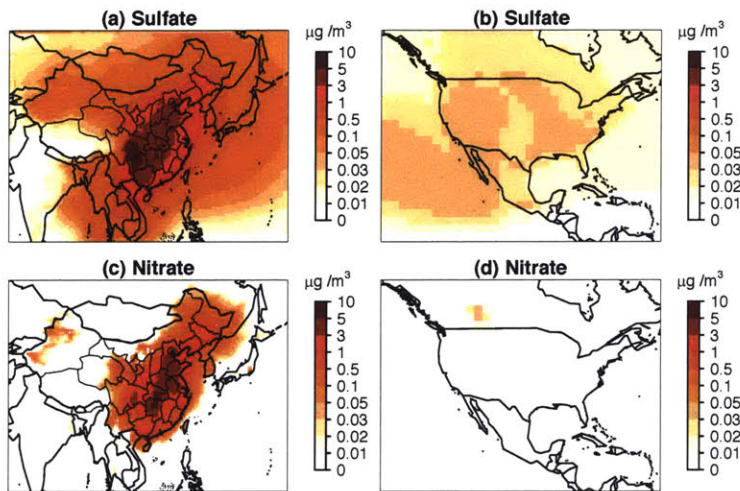
Figure 3.4. Reductions in simulated annual-mean surface concentrations of sulfate (a, b) and nitrate (c, d) under the 4% Policy scenario compared to the No Policy scenario in East Asia and the US in 2030.
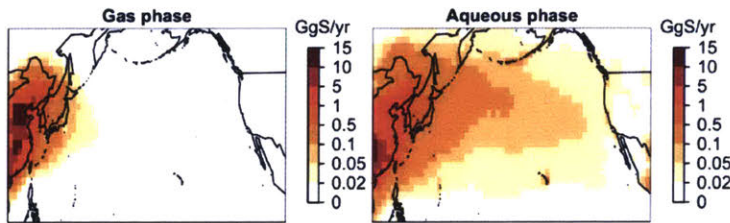
Figure 3.5. Reductions in annual sulfate production below 2km in gas phase and aqueous phase under the 4% Policy scenario compared to No Policy in 2030.

Figure 3.3c and 3.3d shows the reductions in simulated annual-mean surface concentrations in MDA8 ozone under the 4% Policy scenario compared to the No Policy scenario in East Asia and the US in 2030. Following reduction in precursor emissions, the population-weighted MDA8 ozone concentration in China is reduced by 1.6 ppb under the 4% Policy scenario. Co-benefits of MDA8 ozone are higher in Sichuan and Guizhou provinces, and are negative in some areas in North China. Despite NO_x emissions reductions in both North and South China (Figure 3.2b), ozone co-benefits in South China are positive (that is, climate policies result in ozone reductions) throughout the year, but are negative (result in ozone increases) in some places in North China in spring and fall, and negative in most of North China in winter (Figure 3.6a-d). To examine whether the ozone co-benefits are due to reductions in NO_x emissions or other ozone precursors (e.g. NMVOCs and CO), we conducted sensitivity simulations of the 4%

49

Policy scenario in one month of each season — January, April, July, and October, in which only NO_x emissions are changed, while emissions of all the other species follow the No Policy scenario. We found that ozone co-benefits under the 4% Policy case are dominantly due to the reduction in NO_x emissions in every season (Figure 3.7). Compared to the co-benefits in seasonal averages of MDA8 ozone, co-benefits in seasonal averages of 24-hour ozone are similar in pattern, but smaller in magnitude (Figure 3.6e-h).

The direction of the changes in seasonal averages of 24-hour ozone can be explained by whether ozone formation is in a NO_x-limited or NO_x-saturated regime (Sillman, 1995). Ozone is produced from a chain reaction initiated by oxidation of NMVOCs with OH radical,

$$RH + OH + O_2 \rightarrow RO_2 + H_2O \text{ (R1)}$$
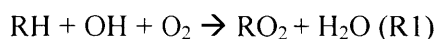
followed by reaction of RO_2 with NO,

$$RO_2 + NO \rightarrow RO + NO_2 \text{ (R2)}$$

$$RO + O_2 \rightarrow R'CHO + HO_2 \text{ (R3)}$$
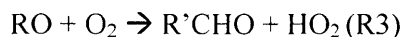
The HO_2 radical then reacts with NO to regenerate OH,

$$NO + HO_2 \rightarrow NO_2 + OH \text{ (R4)}$$

NO_2 is photolyzed to generate atomic oxygen, which combines with O_2 to create O_3,

$$NO_2 + hv \rightarrow NO + O(^3P) \text{ (R5)}$$

$$O(^3P) + O_2 + M \rightarrow O_3 + M \text{ (R6)}$$
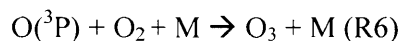
Main radical termination reactions are:

$$HO_2 + HO_2 \rightarrow H_2O_2 + O_2 \text{ (R7)}$$

$$RO_2 + HO_2 \rightarrow ROOH + O_2 \text{ (R8)}$$

$$NO_2 + OH + M \rightarrow HNO_3 + M \text{ (R9)}$$

The division between a NO_x-limited and NO_x-saturated regime depends on the relative abundance of HO_x (OH + HO_2 + RO_2) radicals and NO_x. NO_x-limited regime occurs when peroxides represent the dominant radical sink (R7 and R8). In this case, the rate of ozone formation is determined by the reaction of HO_2 and RO_2 with NO (R2 and R4) and increases with increasing NO_x. NO_x-saturated regime occurs when HNO_3 represents the dominant radical sink (R9). In this case, the rate of ozone formation is determined by the reaction of VOCs with OH (R1). This rate increases with increasing VOCs, but decreases with increasing NO_x because ambient OH decreases in HNO_3 formation (R9).

Previous studies have used the ratio of formaldehyde (HCHO) to nitrogen dioxide (NO_2) as a regime indicator of ozone formation (Sillman, 1995; Martin et al., 2004). This ratio represents the relative abundance of HO_x and NO_x because the oxidation of VOCs often leads to the formation of HCHO and HCHO is a source of HO_x through photolysis:

$$HCHO + hv + 2O_2 \rightarrow 2HO_2 + CO$$
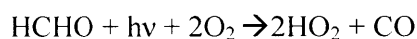
Here we use the regime thresholds of surface ratio of $HCHO/NO_2$ identified by Jin et al. (2017) over East Asia (a ratio <0.5 being NO_x-saturated and >0.8 being NO_x-limited). Supplementary Figure 3.6i-1 shows that South China is in a NO_x-limited regime in all seasons where ozone decreases (or positive co-benefits) as NO_x decreases. North China is primarily in a NO_x-saturated regime in winter, spring, and fall, where ozone increases (or negative co-benefits) when NO_x decreases. Population-weighted co-benefits in South Korea, Japan, and the US under this policy scenario are 0.6, 0.5, and 0.2 ppb, respectively, which are 13-35% of that in China. Ozone co-benefits in the US are higher in the west.
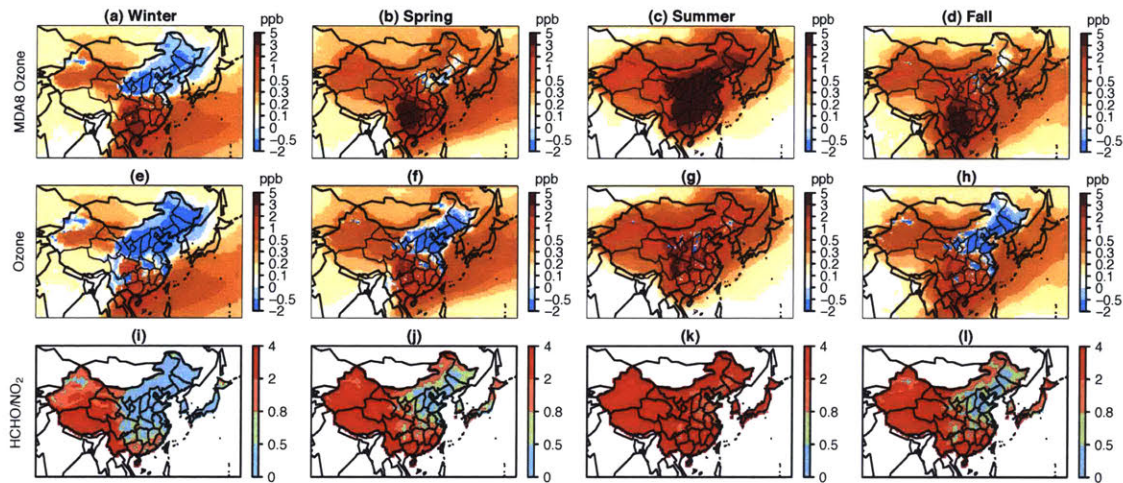
Figure 3.6. Seasonal averages of simulated reductions in MDA8 ozone (a-d) and 24-hour ozone (e-h) under the 4% Policy scenario compared to No Policy, and the surface ratio of HCHO to NO_2 under the No Policy scenario (i-l, only values in China, South Korea, and Japan are shown) in 2030.
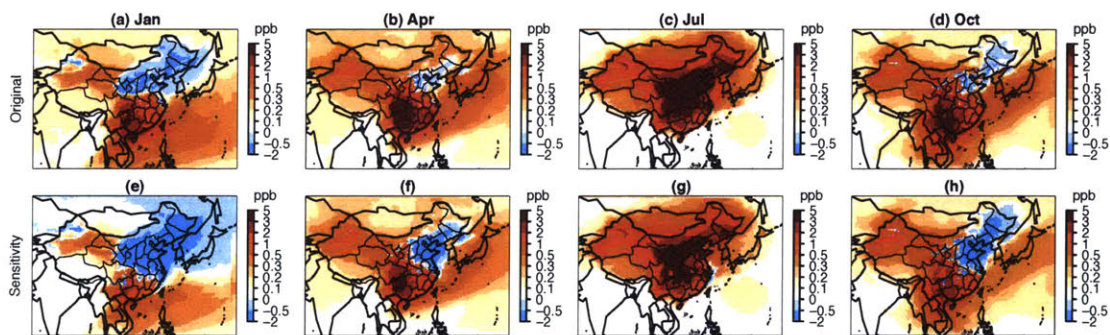
Figure 3.7. Reductions in simulated MDA8 ozone under the 4% Policy scenario compared to No Policy in January, April, July, and October in 2030: (a-d) original simulations, (e-h) sensitivity simulations of the 4% Policy scenario in which only NO_x emissions are changed, while emissions of all the other species follow the No Policy scenario.

3.3.2 Co-benefits under different policy stringencies

Figure 3.8 compares the percentage reductions of $PM_{2.5}$ and ozone in China and its downwind countries to reductions in Chinese CO_2 emissions under different policy stringencies. Li et al. (2018) found that the relative reduction of population-weighted $PM_{2.5}$ at the national level in each scenario is less than proportional to the associated CO_2 reduction (with a regression slope of 0.54) largely because NH_3 emissions are barely affected by climate policy. This linearity also holds for downwind countries, but with smaller slopes of 0.28, 0.18, and 0.02 in South Korea,

52

Japan, and the US, respectively, as different scenarios only change the $PM_{2.5}$ originated from Chinese emissions which is a small fraction of the total $PM_{2.5}$ in each country. Between the two dominant species of $PM_{2.5}$ — sulfate and nitrate, the percentage reductions of nitrate are less than those of sulfate in China (Figure 3.9). This smaller slope of nitrate is due to both a less proportional reduction of NO_x emissions to CO_2 reduction than SO_2 emissions, and a less proportional reduction of nitrate to NO_x emissions than sulfate to SO_2 emissions, especially in winter (Figure 3.10). Relative reductions of ozone are also reduced linearly with CO_2 emissions under different scenarios in these four countries. The regression slope between reductions in ozone and CO_2 emissions in China is 0.14, one fourth of that for $PM_{2.5}$. This is because Chinese anthropogenic emissions only contribute to a small fraction of the total ozone over China, with contributions from natural sources and anthropogenic emissions elsewhere. By conducting a sensitivity simulation in which Chinese anthropogenic emissions of NO_x, CO, and NMVOCs are zeroed out in 2010, we found that this fraction is about 25% averaged over China, consistent with Wang et al. (2011). The slopes in downwind countries decay from 0.06 in South Korea to 0.02 in the US, which is slower than $PM_{2.5}$ due to a longer lifetime of ozone than aerosols.
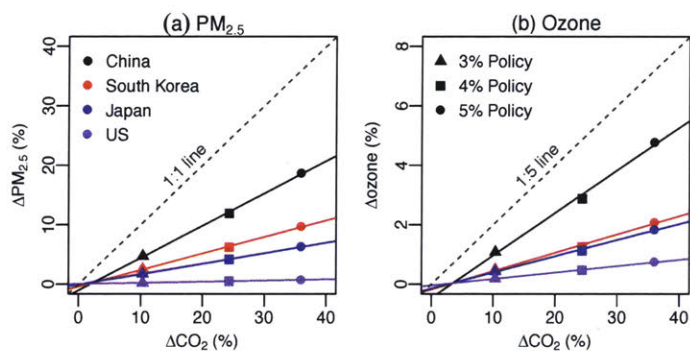
Figure 3.8. Reductions in population-weighted $PM_{2.5}$ (a) and MDA8 ozone (b) concentrations in China and three downwind countries in response to reductions in Chinese CO_2 emissions under climate policy scenarios relative to No Policy in 2030. Both reductions are shown in percentages.
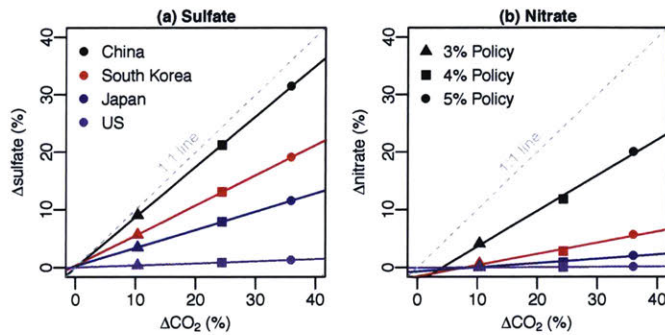
Figure 3.9. Reductions in population-weighted sulfate (a) and nitrate (b) concentrations in response to reductions in Chinese CO_2 emissions under climate policy scenarios relative to No Policy in China and three downwind countries in 2030. Both changes are shown in percentages.
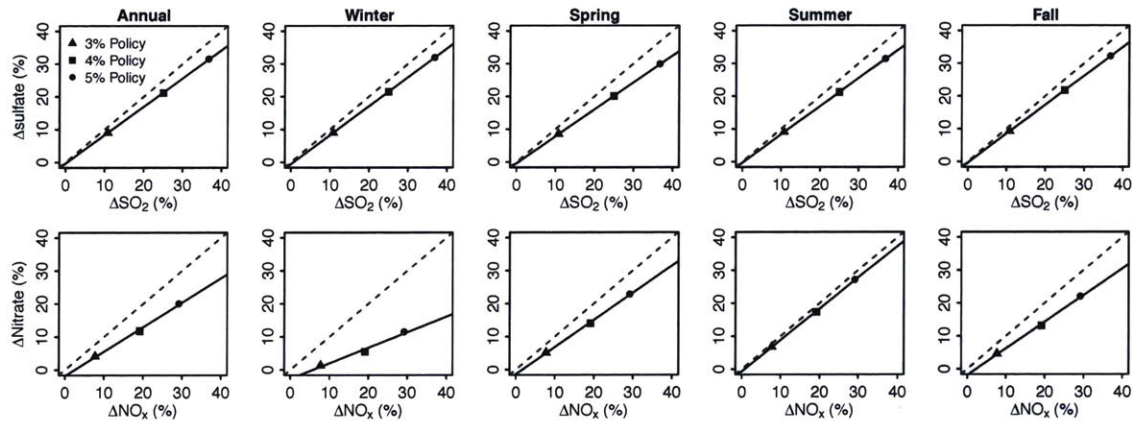
Figure 3.10. Reductions in annual and seasonal averages of population-weighted $PM_{2.5}$ in China in response to reductions in Chinese precursor emissions under climate policy scenarios relative to No Policy in 2030. Top panel: sulfate concentrations to SO_2 emissions, bottom panel: nitrate concentrations to NO_x emissions. Both changes are shown in percentages.

3.3.3 Avoided premature deaths

Table 3.4 listed avoided $PM_{2.5}$- and ozone-related premature deaths of the 4% Policy scenario. Compared to the No Policy scenario, the 4% Policy scenario prevents 95,200 (78,500—112,000; 95% CI) $PM_{2.5}$-related premature deaths in China in 2030. Avoided deaths from $PM_{2.5}$ in South Korea, Japan, and the US are 1,000 (600–1,200), 2,000 (1,400–2,600), and 600 (400–900), respectively, which are two orders of magnitude smaller than those in China. Avoided $PM_{2.5}$-related deaths in Japan double those in South Korea even though the reduction in population-weighted $PM_{2.5}$ in Japan is only 30% of that in South Korea. This is because Japan has an exposed population that is 2.3 times as large as South Korea's, and baseline mortality rates of

IHD, CEV, and LC for Japan are 54-100% higher than those for South Korea (Table 3.2). The 4% Policy scenario also reduces ozone-related premature deaths in China by 54,300 (37,100–71,000; 95% CI), which is nearly 60% of those from $PM_{2.5}$. In contrast, this figure is only 22% using an older CRF from Jerrett et al. (2009). Avoided deaths due to ozone in South Korea are 30% of those from $PM_{2.5}$, much lower than the fraction in China (57%) and Japan (76%), since the baseline incidence rate of ozone-related respiratory disease in South Korea is much smaller (Table 3.2). In contrast, avoided deaths from ozone in the US are double those from $PM_{2.5}$ because of a relatively larger reduction in ozone concentration compared to $PM_{2.5}$ — ozone reduction between China and US differs by a factor of eight, while $PM_{2.5}$ reduction differs by two orders of magnitude (Table 3.3). Avoided premature deaths in the four countries from both $PM_{2.5}$ and ozone also rise proportionally as policy stringency increases (Figure 3.11).

Table 3.4. Avoided $PM_{2.5}$- and ozone-related premature deaths under the 4% Policy scenario compared to the No Policy scenario in China and three downwind countries in 2030. Ozone-related deaths are calculated using two different CRFs. Values in parenthesis represent 95% confidence intervals.

	Population of adults ≥30 years in 2030	Avoided deaths per year			
		$PM_{2.5}$	Ozone (CRF from Turner et al., 2016)	Ozone (CRF from Jerrett et al., 2009)	$PM_{2.5}$ and Ozone (Ozone CRF from Turner et al., 2016)
China	971,139,000	95,200 (78,500—112,000)	54,300 (37,100—71,000)	21,100 (7,000—34,600)	149,400 (125,400—173,300)
South Korea	38,371,000	1,000 (600—1,200)	300 (200—400)	90 (30—150)	1,200 (900—1,600)
Japan	88,977,000	2,000 (1,400—2,600)	1,500 (1,100—2,000)	500 (200—800)	3,500 (2,800—4,300)
US	224,712,000	600 (400—900)	1,300 (800—1,800)	200 (100—400)	1,900 (1,400—2,500)
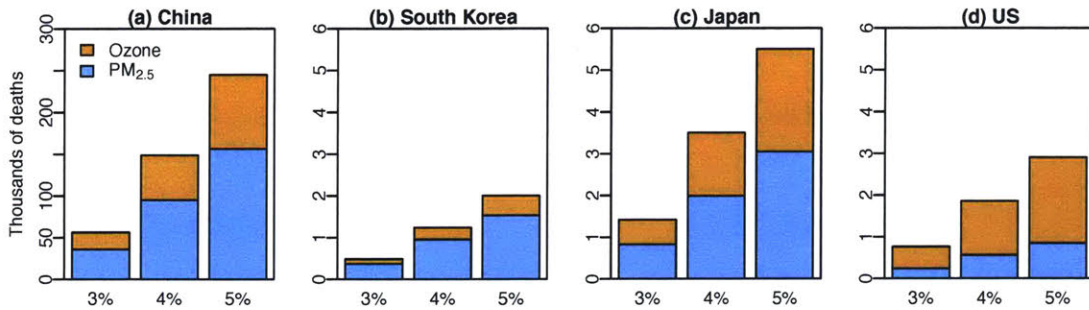
Figure 3.11. Avoided PM$_{2.5}$- and ozone-related premature deaths under three climate policy scenarios relative to No Policy in China (a) and three downwind countries (b-d) in 2030. Ozone-related deaths are calculated using CRF in Turner et al. (2016).

3.4 Discussion and conclusions

We quantify the co-benefits of China's climate policy with three different stringencies on PM$_{2.5}$ and ozone concentrations and their associated health impacts in China and three downwind countries. We find that under a policy scenario consistent with China's pledge to peak CO$_2$ emissions in 2030 (4% Policy scenario), population-weighted concentrations of PM$_{2.5}$ and MDA8 ozone in China would reduce by 8.3 μg/m^3 and 1.6 ppb in 2030 compared to the No Policy scenario. The reduction in ozone prevents 54,300 (95% CI: 37,100–71,000) premature deaths in China in 2030 using a recently updated CRF, 57% of the avoided deaths from PM$_{2.5}$. The 4% Policy scenario also leads to air quality and health co-benefits in downwind countries, with 1,200 (900—1,600), 3,500 (2,800—4,300), and 1,900 (1,400—2,500) premature deaths avoided in South Korea, Japan, and the US, respectively. Total avoided deaths in these three downwind countries are about 4% of those in China. Avoided deaths from PM$_{2.5}$ are more than those from ozone in South Korea and Japan, while ozone is more important in the US. Similar to co-benefits from PM$_{2.5}$ in China, co-benefits from ozone and in downwind countries for both PM$_{2.5}$ and ozone also rise with increasing policy stringency.

Assumptions and model limitations may affect the magnitude of these calculated co-benefits. A newly published study (Burnett et al., 2018) suggested that outdoor PM$_{2.5}$ pollution causes several-fold more deaths than previous estimates; health co-benefits from PM$_{2.5}$ estimated here would be larger if using this CRF. We chose to use the older CRF to enable comparison with previous work for China (Li et al., 2018). Second, recent bottom-up inventory and satellite

56

studies suggested a reduction in Chinese SO_2 and NO_x emissions from 2010 to 2017 by 62% and 17%, respectively (Zheng et al., 2018). Reductions in base-year emissions would reduce calculated co-benefits of sulfate and nitrate proportionally. Finally, the 95% CIs of avoided premature deaths reported here only represent uncertainties in CRF, and recent studies suggested that it may be exceeded by uncertainties from either simulated air pollution among different models (Liang et al., 2018) or climate variability (Saari et al., 2019).

Despite these uncertainties, our study shows that co-benefits of climate policy from reducing ozone-related premature deaths in China are comparable to those from $PM_{2.5}$. Ozone-related co-benefits have often been omitted in previous studies. Further, we found co-benefits from Chinese climate policy outside of China's borders. While avoided premature deaths in transboundary regions are only 4% of those in China, avoided premature deaths of 1,900 in the US from China's climate policy in 2030 in this study is 4-17% of the health co-benefits from climate policy in the US in either 2030 or 2050 (Shindell et al., 2016; Thompson et al., 2014; Y. Zhang et al., 2017).

Chapter 4 Potential changes in the sensitivities of inorganic fine particulate matter to precursor emissions in China

Abstract

This study examines the potential changes in the sensitivities of inorganic $PM_{2.5}$ to precursor emissions in China in response to national reductions in SO_2 and NO_x emissions. Anthropogenic emissions of SO_2 and NO_x are predicted from an energy-economic model with sub-national detail for China (C-REM), and inorganic $PM_{2.5}$ is simulated using an atmospheric chemical transport model GEOS-Chem. Sensitivities are derived from simulations with 10% perturbations in emissions of each precursor nationally. We find that inorganic $PM_{2.5}$ in 2010 is most sensitive to NH_3 emissions in January and more sensitive to SO_2 and NO_x emissions in July. Under scenarios that reduce SO_2 and NO_x emissions, sensitivities to SO_2 and NO_x emissions would increase, but sensitivity to NH_3 emissions would decrease in January and July. The largest absolute changes in sensitivities are found in January for NO_x and NH_3.

4.1 Introduction

Fine particulate matter with a diameter of 2.5 microns or less ($PM_{2.5}$) can penetrate deeply into lungs and circulatory system, causing respiratory and cardiovascular diseases. China has the highest $PM_{2.5}$ concentrations in the world, and inorganic $PM_{2.5}$, including sulfate, nitrate, and ammonium, is a major component of $PM_{2.5}$ in China. Inorganic $PM_{2.5}$ is formed in the atmosphere through complex and non-linear chemical processes from its precursors —sulfur dioxide (SO_2), nitrogen oxides (NO_x), and ammonia (NH_3). Because emissions of these precursors come mostly from human activities, previous studies have examined how inorganic $PM_{2.5}$ responds to changes in emissions of each precursor, i.e. sensitivity of $PM_{2.5}$ to emissions, to help better design pollution control policies (Ansari and Pandis, 1998; Pinder et al., 2007). China has enforced regulations to control air pollutants, which has led to a large reduction in

SO_2 emissions since 2006 and a small reduction in NO_x emissions since 2012 (Zhao et al., 2013; Zheng et al., 2018). As China's SO_2 and NO_x emissions continue to decrease, sensitivities of inorganic $PM_{2.5}$ to further emission reductions could change. In this study, we examine the potential changes in the sensitivities of inorganic $PM_{2.5}$ to precursor emissions under three emission control scenarios compared to 2010.

The current sensitivities of $PM_{2.5}$ to precursor emissions in China have been examined using different methods, including finite difference methods and adjoint modeling (Wang et al., 2011; Kharol et al., 2013; Lee et al., 2015). These studies suggested that comparisons of sensitivities to the three precursors vary by season and by region. Wang et al. (2011) examined sensitivities in three industrialized regions of eastern China in 2005 using the Community Multiscale Air Quality model, with sensitivities defined as relative changes in $PM_{2.5}$ to relative changes in emissions for a 10% reduction in precursor emissions. They found that January $PM_{2.5}$ is most sensitive to NH_3 emissions in the Yangtze River delta and Pearl River delta, but more sensitive to SO_2 and NO_x emissions in the North China Plain, while largest sensitivities to SO_2 are found in July for all three regions. By comparing changes in inorganic $PM_{2.5}$ concentration due to a 10% increase in SO_2, NO_x, or NH_3 emissions nationally using GEOS-Chem, Kharol et al. (2013) found that inorganic $PM_{2.5}$ in 2006 is most sensitive to NH_3 emissions in winter, but more sensitive to SO_2 and NO_x emissions in other seasons. Lee et al. (2015) calculated sensitivities of global $PM_{2.5}$-related premature deaths to emissions of precursor gases and primary carbonaceous aerosols using GEOS-Chem adjoint model, and found that a 1 kg km−2 yr−1 decrease in NH_3 emissions in China would lead to the largest reductions in global mortality.

China plans to continue controlling SO_2 and NO_x emissions, and the 13th Five-Year Plan mandates 15% reductions in both SO_2 and NO_x emissions between 2015 and 2020. In addition to end-of-pipe control polies like scrubbing, climate or energy policies that limit fossil fuel combustion can also reduce SO_2 and NO_x emissions. China has committed to achieve a national peak of CO_2 emissions by 2030, resulting in potentially large air quality co-benefits (Li et al. 2018). Projections of SO_2 and NO_x emissions under four Representative Concentration Pathways (RCP) used in the IPCC AR5 report projected similar trends for in China, which peak around 2020 and decrease dramatically to 2100 because of similar assumptions in emissions control policies used in all scenarios (van Vuuren et al., 2011). Other China-specific studies

projected that SO_2 and NO_x emissions are more likely to decrease with reduction degree depending on the stringency of energy and emission control policies (S. Wang et al., 2014; Zhao et al., 2014). NH_3 emissions come mostly from agricultural activities like fertilizer and livestock waste, and their estimation and future trends are more uncertain. China's Ministry of Agriculture announced an action plan to limit annual increases in fertilizer use to 1% from 2015 to 2019, and to prohibit further increases beyond 2020. NH_3 emissions in China under RCP scenarios projected a small and steady increasing trend from 2000 to 2100 (van Vuuren et al., 2011).

Sensitivities of inorganic $PM_{2.5}$ to precursor emissions can change as a result in large-scale emission reductions through altering the chemical regime of nitrate formation and levels of oxidants. A large reduction in SO_2 and NO_x emissions from 2005 to 2012 in the US was found to result in an increase in the sensitivity to SO_2 emissions year-round and to NO_x emissions in winter, yet a decreased sensitivity to NH_3 emissions (Holt et al., 2015). Fu et al. (2017) found that reductions of China's SO_2 and NO_x emissions by 45% would result in a lower sensitivity of PM reduction to NH_3 emissions control. However, changes in sensitivities to SO_2 and NO_x emissions were not examined in that study.

Here we examine potential changes in the sensitivities of $PM_{2.5}$ to three precursor emissions under three emission control scenarios compared to 2010. Future emissions are projected under three emission scenarios consistent with the carbon policy that can achieve China's commitment on CO_2 emissions in 2030, with different levels of end-of-pipe emission control policies. We find that under SO_2 and NO_x emissions declines in China, sensitivity to NH_3 emissions decreases, but sensitivities to SO_2 and NO_x emissions increase.

4.2 Methods

We project anthropogenic emissions of SO_2 and NO_x through 2030 using an energy-economic model at provincial level in China, the China Regional Energy Model (C-REM). We simulate three emission control scenarios that have the same level of carbon policy that could achieve China's commitment to peak CO_2 emissions in 2030 and different levels of end-of-pipe control policy (denoted as EC1, EC2, and EC3 from the least to the most stringent scenario). $PM_{2.5}$ under the three scenarios is simulated using the nested-grid GEOS-Chem model for East Asia.

61

We further conduct sensitivity simulations with 10% perturbations (increase and decrease) in SO_2, NO_x, and NH_3 emissions nationally for 2010 and EC3. These simulations are conducted in January and July, representing winter and summer conditions.

4.2.1 Emission projections

C-REM is a global computable general equilibrium model that resolves China's economy and energy system at the provincial level, including production, consumption, interprovincial and international trade, energy use, and emissions of CO_2 and air pollutants. Emissions of air pollutants by province, sector and energy type are calculated from projected energy use (for combustion sources) or economic activity (for non-combustion sources), multiplied by corresponding emissions factors. Emissions factors in 2007 are derived from emissions reported in the Regional Emission Inventory in Asia (REAS, Kurokawa et al., 2013), and are calibrated to 2010 and 2015 based on national total emissions in 2010 and 2012 reported from the Multi-resolution Emission Inventory for China (MEIC: http://www.meicmodel.org). Emission factors are calculated under different scenarios to decrease exponentially after 2015 to account for new emission control measures and improvement on existing ones following the methodology in Webster et al. (2008). We simulate three scenarios which have the same level of carbon policy but different levels of end-of-pipe control policy. Carbon policy is implemented through a carbon price that leads to a 4% per year reduction in CO_2 intensity between 2015 and 2030 and a peak of CO_2 emissions in 2030. Different levels of end-of-pipe control policy are simulated by varying exponential decay parameters. Table 4.1 shows the decay parameters for SO_2 and NO_x under the three scenarios. Decay parameters under EC1 are from Webster et al. (2008), which are determined based on historical emission trends in 15 developed countries. The decay parameter for SO_2 is three times than that for NO_x. We generate the two more aggressive scenarios (denoted as EC2 and EC3) by doubling and tripling the decay parameters in EC1, respectively. Further details about C-REM, matching of sectors and energy type between C-REM and REAS, calibration in 2010 and 2015 with MEIC, and effects of the exponential decay on emission projections are provided by Li et al. (2018). Gridded emissions in 2010 and in 2030 under the three scenarios, used as input to GEOS-Chem, are derived by scaling gridded emissions from REAS in 2007 based on provincial-level emissions of SO_2 and NO_x from C-REM in 2007, 2010, and 2030. Other emissions are kept the same at current levels for all the

simulations. For NH_3 emissions, we use the inventory from Streets et al. (2003) with a 30% reduction nationwide as suggested by Huang et al. (2012) and seasonal variation implemented by Fisher et al. (2011).

Table 4.1. Exponential decay parameters in emission factors for SO_2 and NO_x under three scenarios (unit: per year).

	SO_2	NO_x
EC1	-0.03	-0.01
EC2	-0.06	-0.02
EC3	-0.09	-0.03

4.2.2 GEOS-Chem simulation

We use GEOS-Chem v9-01-03 to conduct nested-grid simulations at $0.5° \times 0.667°$ resolution over East Asia ($11°S–55°N$, $70–150°E$; Wang et al., 2004). GEOS-Chem simulates detailed NO_x-VOC-ozone-aerosol tropospheric chemistry (Park et al. 2004). Gas-aerosol phase partitioning of sulfate-nitrate-ammonium aerosols is computed with the ISORROPIA II thermodynamic module (Fontoukis and Nenes, 2007; Pye et al., 2009). Each simulation is one month long with a two-month spin-up period that uses meteorological fields of either November 2009 to January 2010 or May 2010 to July 2010. We use a scaling factor of 1.33 to convert dry aerosol concentrations from GEOS-Chem outputs to observed $PM_{2.5}$ which is often under a relative humidity of 35% (Chow and Watson, 1998). We compared simulated annual-average concentrations of sulfate, nitrate and ammonium in 2007 with observations at 16 sites in China from 2006 to 2007 (Zhang et al. 2012), including 9 rural sites and 7 urban sites (Figure 4.1). The model reproduces the spatial distribution of all three species with correlation coefficient (R) greater than 0.8, but is likely subject to systematic biases. Sulfate concentrations at the rural sites are underestimated by 34%. Simulated nitrate concentration at Gaolanshan, a rural site in Gansu province in northwestern China, is 9 times the observed level. If this abnormal site is excluded, nitrate concentrations at the rural sites are overestimated by 50%. In contrast, the model tends to underestimate sulfate and nitrate at urban sites by 42% and 24%, respectively. This is because our model with a resolution of $0.5° \times 0.667°$ cannot capture the spatial heterogeneity in emissions, meteorology and chemistry at urban scale (e.g. Y. Wang et al. 2014).

We further discussed the implications of the potential underestimation of sulfate and overestimation of nitrate in Section 4.4.
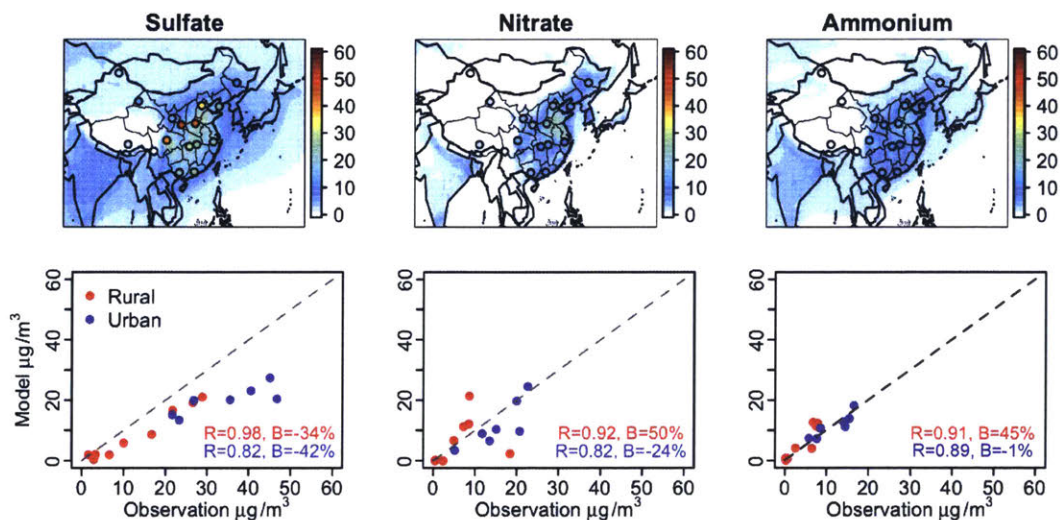
Figure 4.1. Comparison between simulated inorganic PM$_{2.5}$ and observations. Top panel: simulated annual-average concentrations over East Asia in 2007. Circles indicate locations and concentrations of observations. Bottom panel: scatterplot of simulated and observed annual-average concentrations at 9 rural sites and 7 urban sites. Correlation coefficient (R) and normalized mean bias (B) for rural and urban sites are shown in inset.

4.2.3 Sensitives of inorganic PM$_{2.5}$ to emissions

The sensitivities of inorganic PM$_{2.5}$ to each precursor in 2010 and EC3 are calculated as the difference in population-weighted PM$_{2.5}$ concentration between the two emission perturbation simulations divided by the difference in national emissions:

$$S_{i,j,k} = \frac{C_{1.1E_{i,j,k}} - C_{0.9E_{i,j,k}}}{0.2E_{i,j,k}}$$

Where i represents precursor (SO$_2$, NO$_x$, or NH$_3$), j represents month (January or July), k represents scenario (2010 or EC3). $E_{i,j,k}$ is the national emissions of precursor i in month j under scenario k in giga-mole (10^9 mole, Gmol) per month, and $c_{1.1Ei,j,k}$ and $c_{0.9Ei,j,k}$ are the simulated population-weighted concentrations of inorganic PM$_{2.5}$ from the corresponding perturbation simulations in µg/m^3. Here we use population-weighted concentrations a proxy for the health effects of PM$_{2.5}$.

64

4.3 Results and Discussion

4.3.1 Emissions changes

Figure 4.2 shows absolute and relative changes of SO_2 and NO_x emissions between 2010 and 2030 under EC3. SO_2 and NO_x emissions are lower than 2010 levels in all three scenarios. SO_2 reduces more than NO_x since SO_2 has larger exponential decay parameters than NO_x (Table 4.1). Under the least stringent scenario EC1, national SO_2 emissions reduce by 10% compared to 2010, while NO_x emissions are nearly the same. In comparison, SO_2 and NO_x emissions under EC3 decrease by 63% and 26%, respectively. Regionally, North China has the largest reductions of SO_2 and NO_x emissions in both absolute and relative terms due to the effects of the underlying carbon policy. Under EC3, SO_2 emissions decrease by 66% in North China, compared to a 61% reduction in South China and a 54% reduction in Sichuan Basin (region boundaries of North China, South China, and Sichuan Basin are shown in Figure 4.2(a)). NO_x emissions even increase in Chongqing, Yunnan, and Jiangxi provinces under EC3 despite a decrease in national emissions. Table 4.2 shows the national total emissions of three precursors in January and July for 2010. Total SO_2 and NO_x emissions in July are slightly higher than those in January by 1% and 3%, respectively. Total NH_3 emissions in July are three times those in January.

65
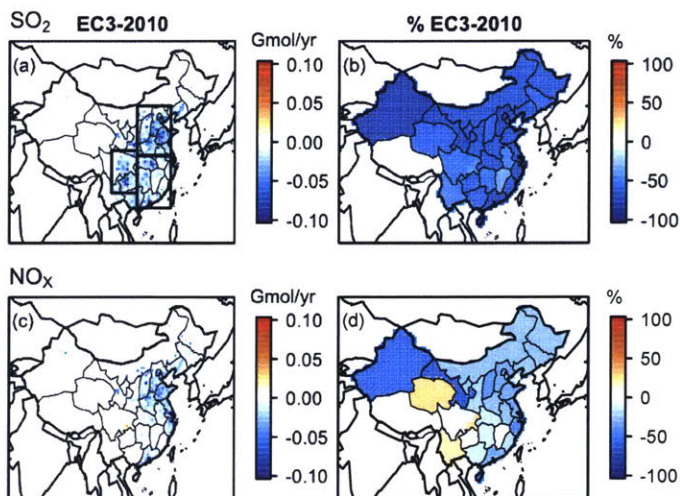
Figure 4.2. Absolute and relative changes of SO_2 and NO_x emissions between 2010 and EC3. Rectangles in (a) represent North China (109.67-120.33°E, 32.25-42.25°N), South China (109.67-120.33°E, 21.75-32.25°N), and Sichuan Basin (101.67-109.67°E, 24.75-33.25°N).

Table 4.2. China's national anthropogenic emissions of SO_2, NO_x, and NH_3 in January and July for 2010 and EC3 (unit: Gmol/month).

	2010		EC3	
	January	July	January	July
SO_2	36.9	37.1	13.9	14
NO_x	49.7	51.1	36.9	37.8
NH_3	20.3	64.1	20.3	64.1

4.3.2 Changes in inorganic $PM_{2.5}$ concentrations

Table 4.3 shows the population-weighted concentrations of inorganic $PM_{2.5}$ in January and July for 2010 and EC3, and Figure 4.3 shows the spatial distribution of absolute changes in concentrations under EC3 compared to 2010 in January and July. In response to a national reduction in SO_2 emissions by 63% and a reduction in NO_x emissions by 26% under EC3, the national population-weighted concentration of inorganic $PM_{2.5}$ in January only reduces by 10%, from 59.6 to 53.9 $\mu g/m^3$. This is due to a large reduction in sulfate by 8.4 $\mu g/m^3$ (52%), offset by an increase in nitrate of 4.1 $\mu g/m^3$ (14%). Absolute changes in sulfate and nitrate are both higher in South China and Sichuan Basin than North China (Figure 4.3). In contrast, July $PM_{2.5}$ reduces by 29% (from 43.6 to 28.3 $\mu g/m^3$) with reductions in both sulfate (7.7 $\mu g/m^3$ and 58%) and nitrate (3.8 $\mu g/m^3$ and 19%). Absolute reductions are higher in North China than South

66

China and Sichuan Basin. Nitrate concentration shows a slight increase in Chongqing (Figure 4.3).
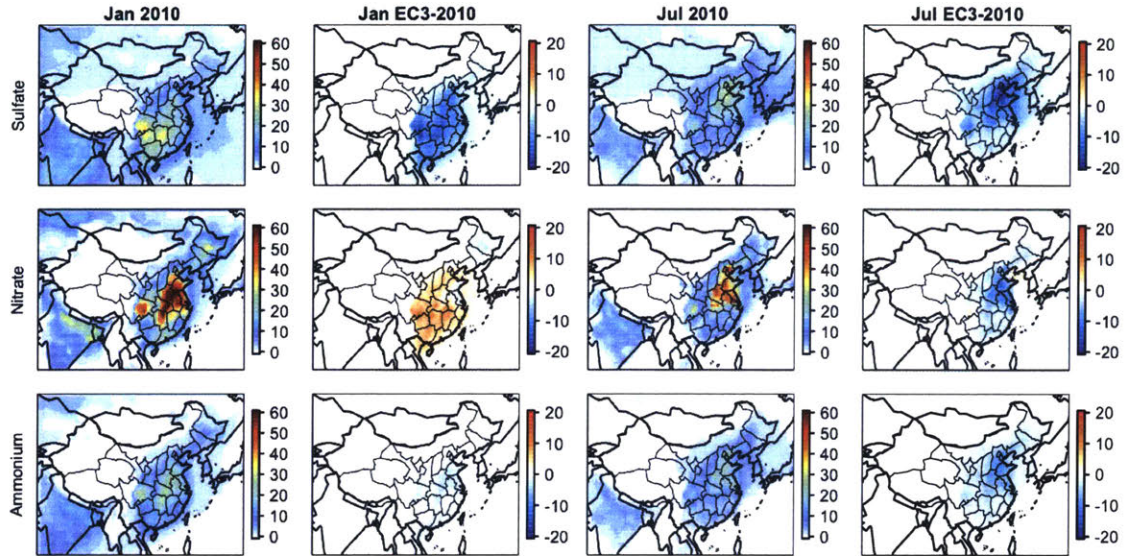
Figure 4.3. Simulated sulfate, nitrate, ammonium concentrations in 2010, and changes of concentrations under the EC3 scenario compared to 2010 in January and July (in unit of $\mu g/m^3$).

Figure 4.4 shows the percentage changes in population-weighted sulfate/nitrate concentrations under the three scenarios relative to 2010 versus percentage changes in national SO_2/NO_x emissions. This comparison illustrates how each component of $PM_{2.5}$ changes proportionally relative to its precursor, under the emissions scenarios where both SO_2 and NO_x are changing simultaneously. Sulfate reduces linearly with reductions in SO_2 emissions. The linear regression slopes are 0.84 and 0.92 in January and July, respectively, meaning that proportional changes in sulfate concentration are a bit less than those in SO_2 emissions. For example, SO_2 emissions decrease by 42% under EC2, and sulfate only decrease by 34% in January. Relative reductions between NO_x emissions and nitrate concentrations are linear in July with a linear regression slope of 0.78. However, nitrate concentration increase from 2010 to EC3, and the increase becomes saturated between EC2 and EC3.
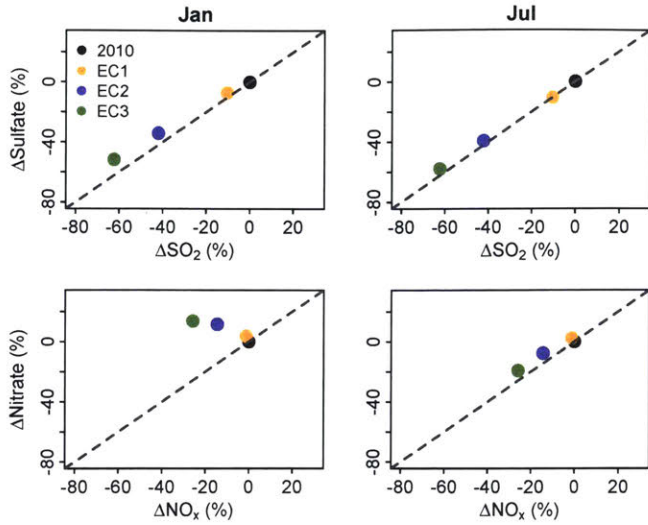
Figure 4.4. Percentage changes in national population-weighted PM$_{2.5}$ concentrations between 2010 and the three scenarios versus corresponding percentage changes in national emissions of selected precursors in China in January and July, under emission scenarios where SO$_2$ and NO$_x$ are changing simultaneously. Top panel shows sulfate versus SO$_2$, and bottom panel shows nitrate versus NO$_x$. Grey dashed lines represent the 1:1 line.

4.3.3 Changes in sensitivities of inorganic PM$_{2.5}$ to each precursor

Figure 4.5 shows the sensitivities of population-weighted inorganic PM$_{2.5}$ and its speciation to each precursor in January and July for 2010 and EC3. Sulfate has the largest sensitivity to SO$_2$ in both months. Nitrate in January is most sensitive to NH$_3$ and has a negative sensitivity to SO$_2$ (meaning an increase in SO$_2$ emissions would reduce nitrate). Nitrate in July has the highest sensitivity to NO$_x$. These sensitivities can help to explain the nitrate increase shown in Section 3.2, as changes in nitrates concentrations between can be expressed as:

$$\Delta c = \int_{E_{SO2,2010}}^{E_{SO2,EC3}} \frac{\partial c}{\partial E_{SO2}} dE_{SO2} + \int_{E_{NOx,2010}}^{E_{NOx,EC3}} \frac{\partial c}{\partial E_{NOx}} dE_{NOx}$$

Sensitivities calculated here are estimates of $\frac{\partial c}{\partial E_{SO2}}$ and $\frac{\partial c}{\partial E_{NOx}}$ at lower and upper limits of emissions (2010 and EC3). The negative sensitivity of nitrate to SO$_2$ in January stays relatively constant when emissions reduce from 2010 to EC3 at -0.26 µg/m^3/Gmol, thus a reduction in SO$_2$ emissions of 26 Gmol/month from 2010 to EC3 (Table 3.2) would lead to an increase in nitrate by about 6 µg/m^3. Although the positive sensitivity of nitrate to NO$_x$ has a similar magnitude compared to SO$_2$ and is increasing as emissions change, NO$_x$ emissions only reduce

by 13 Gmol/month from 2010 to EC3, thereby only offset the nitrate increase by about half, resulting in a nitrate increase by 4 $\mu g/m^3$.

Total inorganic $PM_{2.5}$ in January is most sensitive to NH_3 emissions in 2010 (1.92 $\mu g/m^3$/Gmol). Sensitivity to NH_3 is 10 and 15 times as large as that to NO_x and SO_2, respectively. In contrast, $PM_{2.5}$ in July is more sensitive to SO_2 and NO_x emissions (0.34 and 0.45 $\mu g/m^3$/Gmol), and 40-90% higher than the sensitivity to NH_3 emissions (0.24 $\mu g/m^3$/Gmol). NH_3 sensitivity in July is one order of magnitude lower than that in January. Under EC3 when SO_2 and NO_x emissions reduce by 60% and 30%, NO_x sensitivity increases by 0.33 $\mu g/m^3$/Gmol (nearly a factor of three), while NH_3 sensitivity decreases by 0.48 $\mu g/m^3$/Gmol (25%). Changes in sensitivities of nitrate are the largest among the three aerosol species, accounting for 81% and 66% of the total changes for NO_x and NH_3 emissions. SO_2 sensitivity increases slightly by 30%. NH_3 remains to be the most sensitive precursor for January $PM_{2.5}$ under EC3, but its sensitivity is only 3 times that to NO_x. Changes of sensitives in July have similar directions with those in January. SO_2 and NO_x sensitivities increase (30% and 20%), while NH_3 sensitivity decreases (50%). Again, these changes are dominated by changes in sensitivities of nitrate. However, absolute changes in July (around 0.1 $\mu g/m^3$/Gmol for all three precursors) are much smaller than those in January.
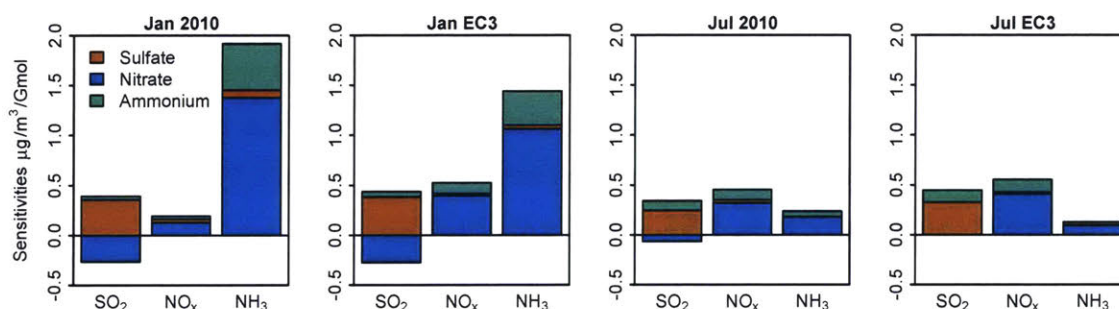
Figure 4.5. Sensitivities of national population-weighted inorganic $PM_{2.5}$ to national emissions of each precursor (SO_2, NO_x, or NH_3) under 2010 and EC3 in January and July.

4.3.4 Chemical mechanisms

In this section, we investigated the chemical mechanisms to explain the changes in $PM_{2.5}$ sensitivities. Gaseous SO_2 and NO_x are first oxidized to sulfuric acid (H_2SO_4) and nitric acid (HNO_3). The thermodynamic module in GEOS-Chem (ISORROPIA II) assumes that species

exist in metastable state, i.e. liquid phase (Fountoukis and Nenes, 2007). H_2SO_4 is nonvolatile and very soluble, thus always forms an aqueous aerosol. The first dissociation of sulfuric acid forms bisulfate (HSO_4^-), which is assumed to be complete in ISORROPIA II (Fountoukis and Nenes, 2007):

$$H_2SO_4 \rightarrow H^+ + HSO_4^-$$

HSO_4^- then dissociates to SO_4^{2-}:

$$HSO_4^- \leftrightarrow H^+ + SO_4^{2-}$$
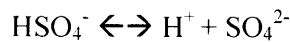
The relative abundance of HSO_4^- and SO_4^{2-} depends on the amount of NH_3, which can dissolve in aerosol forming ammonium (NH_4^+):

$$NH_3(g) \leftrightarrow NH_3(aq)$$

$$NH_3(aq) + H_2O(aq) \leftrightarrow NH_4^+ + OH^-$$
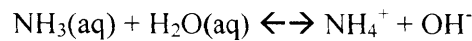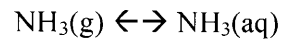
Sulfate represents the total of HSO_4^- and SO_4^{2-}. If there is excessive NH_3 left after neutralizing sulfate, HNO_3 can be taken up by aerosol forming nitrate (NO_3^-):

$$HNO_3(g) \leftrightarrow HNO_3(aq) \leftrightarrow NO_3^- + H^+$$
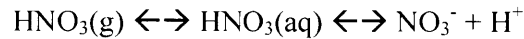
The gas-aerosol phase partitioning of NH_3 and HNO_3 is based on the ambient temperature and relative humidity and the concentrations of sulfate, total ammonia, total nitrate in both gas and aerosol phase. Chemical regimes for nitrate formation can be identified by the gas ratio (GR) defined as (Ansari and Pandis, 1998; Paulot et al., 2014):

$$GR = \frac{c(TNH_3) - 2c(TSO_4)}{c(TNO_3)}$$

Where TSO_4 represents sulfate, TNO_3 and TNH_3 represent total nitrate and total ammonia, i.e. $TSO_4 = HSO_4^- + SO_4^{2-}$, $TNO_3 = HNO_3 + NO_3^-$, $TNH_3 = NH_3 + NH_4^+$. c represents concentration in $\mu mol/m^3$.

When GR>1, defined as NH_3-saturated regime, TNH_3 can fully neutralize both sulfate and TNO_3. In this case, nitrate is sensitive to NO_x emissions rather than NH_3 emissions. When

0<GR<1, defined as NH_3-limited regime, sulfate is fully neutralized but TNO_3 is not. Nitrate has a negative sensitivity to SO_2 emissions as increase in sulfate would decrease nitrate concentration, and it is sensitive to NH_3 emission rather than NO_x emission. When GR<0, TNH_3 is not enough to fully neutralize sulfate (exists as a mixture of HSO_4^- and SO_4^{2-}). Figure 4.6 shows the distribution of daily-average gas ratio for all grid cells in East China (101.67-120.33°E, 21.75-42.25°N) in January and July under 2010 and EC3. There are a total of 35588 samples in each plot (31 days for each of 1148 grid cells). Conditions where GR<0 are rare under all cases (0.2-10.6%). In January 2010, daily-average conditions in East China are dominated by NH_3-limited regime (73%), thus population-weighted nitrate concentration in China has a negative sensitivity to SO_2 emissions and a large positive sensitivity to NO_x. The percentage that fall in the NH_3-limited regime decreases to 59% under EC3, leading to a lower sensitivity to NH_3 emissions and a higher sensitivity to NO_x emissions. On the contrary, NH_3-saturated is the dominated regime in July 2010 (70%) since NH_3 emission in July are three times the level in January, thus nitrate is more sensitive to NO_x than NH_3 in this month. The percentage increases to 90% under EC3, resulting in a greater difference between them.
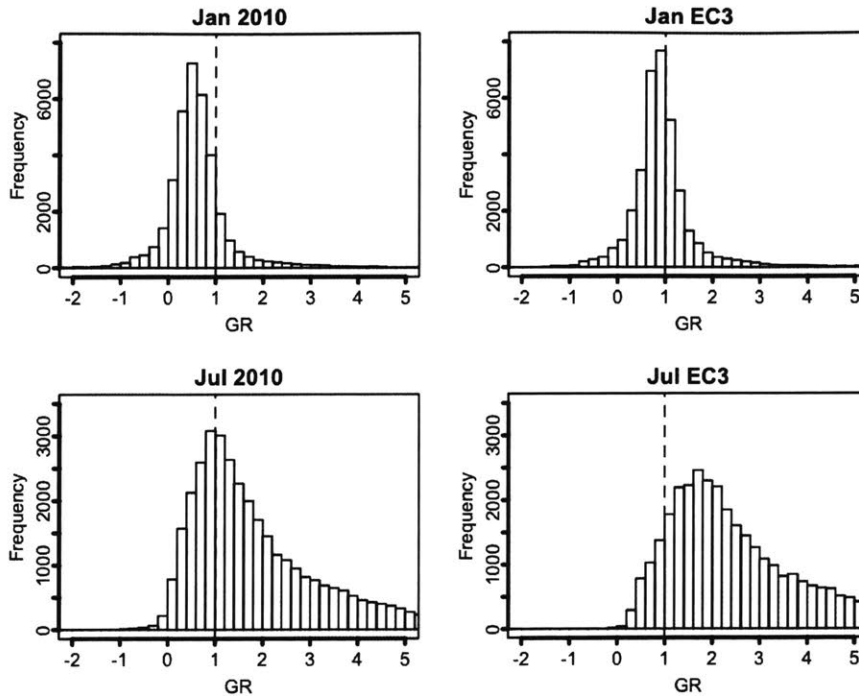
Figure 4.6. Histogram plots of daily-average gas ratio for grid cells in East China (101.67-120.33°E, 21.75-42.25°N) in January and July under 2010 and EC3. Each plot has a total of 35588 samples (31 days for each of 1148 grid cells) with a bin size of 0.2.

4.4 Discussion and conclusions

We find that population-weighted inorganic $PM_{2.5}$ in China in 2010 is most sensitive to NH_3 emissions in January and more sensitive to SO_2 and NO_x emissions in July, consistent with the findings of Kharol et al. (2013). When national SO_2 and NO_x emissions reduce by up to 60% and 30%, respectively, sulfate concentrations decrease proportionally to reduction in SO_2 emissions, but nitrate concentrations increase in January. Meanwhile, sensitivities to SO_2 and NO_x emissions increase, yet sensitivity to NH_3 emissions decreases for both seasons. Absolute changes of sensitivities in January are much higher than those in July, with an increase in NO_x sensitivity by 0.33 $\mu g/m^3$/Gmol and a decrease in NH_3 sensitivity by 0.48 $\mu g/m^3$. The reduction in NH_3 sensitivity is consistent with Fu et al. (2017). A recent emission inventory reported that China's SO_2 and NO_x emissions have decreased by 62% and 17% between 2010 and 2017

(Zheng et al., 2018), similar to the emission reductions under EC3, suggesting that sensitivities may have already changed.

Our sensitivities are subject to model biases including the model's well-documented overestimate of nitrate, and underestimate of sulfate. The positive nitrate bias in GEOS-Chem is also recognized by previous studies in the US (e.g. Heald et al. 2012). Several possible solutions have been suggested, including faster dry deposition of HNO_3 and higher uptake of N_2O_5 on aerosols (Shah et al., 2018) as well as updated wet scavenging processes (Luo et al., 2019). This nitrate bias would increase the absolute sensitivity to NO_x emissions, but unlikely to alter the relative changes in sensitivity from 2010 to EC3. Several studies have found that the underestimate of sulfate in winter haze events may be due to the lack of heterogeneous uptake of SO_2 on aerosols, and suggested different reaction pathways, including by NO_2 and formaldehyde (e.g. Y. Wang et al. 2014; Cheng et al. 2016; Song et al. 2019).

Sensitivities calculated here are at national scale with perturbations in national emissions. Sensitivities at finer scale could be derived from simulations perturbing the emissions of that particular region. Zhao et al. (2017) examined the sensitivities in the Beijing-Tianjin-Hebei region using a similar but improved approach to Wang et al. (2011). They found a negative sensitivity of $PM_{2.5}$ to NO_x emissions, contrary to the positive sensitivity in the larger region of North China Plain found in Wang et al. (2011). Sensitivity of a defined variable, such as averaged concentrations or premature deaths in a region, to emissions in each grid cell can be computed efficiently using adjoint modeling, as done in the global study by Lee et al. (2015). A study examining how the sensitivities would change at city to provincial levels using either approach is worth doing.

Sensitivities in this study are defined as absolute changes in population-weighted concentration per unit number changes in national emissions (i.e. Gmol/month). Other studies have defined sensitives per unit mass changes in emissions or relative changes for both concentrations and emissions. We choose to use the absolute change due to its policy relevance, as it can be straightforwardly combined with future information on costs, as described below. Using other definitions would change the relative comparison among three precursors, but would not affect the relative changes in sensitivities from 2010 to EC3.

Our study suggests that controlling NH_3 emissions in winter may be more effective in reducing $PM_{2.5}$ than controlling SO_2 and NO_x emissions. Studies in the US showed that this strategy could be cost-effective (Pinder et al. 2007). Although anticipated decreases in SO_2 and NO_x emissions would decrease the relative difference between NH_3 and NO_x sensitivity from one magnitude to a factor of three, but the marginal cost of NO_x control is expected to increase as the increasing level of emission reduction. The cost curve of control policies in China is still an area that needs more research. Future studies that combine detailed cost information with sensitivities presented here could provide suggestions to design cost-effective policy. In addition, Liu et al. (2019) suggested that a potential side-effect of controlling NH_3 emission by aggravating acid rain could partly offset the economic benefit from reduced $PM_{2.5}$ and nitrogen deposition, which should also be considered in the cost-benefit analysis.

Chapter 5 Conclusion

$PM_{2.5}$ and ozone are air pollutants that harm human health, and are formed from precursors emitted largely from human activities. These emissions can be reduced at emitting sources by end-of-pipe control policies or as co-benefits of climate policies that limit fossil fuel. Identifying cost-effective control strategies requires understanding relevant policy costs, chemical non-linearities in pollution formation, and the value of health benefits. As the largest CO_2 emitting country with severe air pollution, China has been enforcing regulations to control SO_2 and NO_x emissions, and recently pledged to peak CO_2 emissions in approximately 2030 under the Paris Agreement. This thesis aims to understand the impacts of both carbon and air pollutant policies in China on air pollution and human health.

Chapter 2 quantifies the air quality co-benefits of China's climate policy under three stringencies, and their monetized health co-benefits are compared to climate policy's economic costs. The effects of an illustrative climate policy, a price on CO_2 emissions, are simulated. In a policy scenario consistent with China's recent pledge to peak CO_2 emissions by 2030 (4% Policy scenario), national population-weighted $PM_{2.5}$ concentrations would decrease by 12% in 2030 compared to the No Policy scenario which would prevent 94,000 premature mortalities. Most of the co-benefits are from reductions in inorganic aerosols. The monetized national health co-benefits can partially or fully offset policy costs depending on chosen health valuation. Air quality co-benefits would rise with increasing policy stringency.

Using model simulations performed in Chapter 2, Chapter 3 further quantifies the co-benefits from ozone in China and from both pollutants in three downwind countries. Under the 4% Policy scenario, the avoided deaths from ozone reduction in China are nearly 60% of those from $PM_{2.5}$. This would further increase the monetized health co-benefits in Chapter 2 by 60%. Avoided premature deaths from both pollutants in South Korea, Japan, and the US are 1,200 (900—1,600), 3,500 (2,800—4,300), and 1,900 (1,400—2,500), respectively. Total avoided deaths in these three downwind countries are about 4% of those in China.

Chapter 4 explores the chemical non-linearities in inorganic $PM_{2.5}$ and examines specifically the potential changes in the sensitivities of inorganic $PM_{2.5}$ to precursor emissions due to large

75

scale reductions of SO_2 and NO_x emissions in China. We find that population-weighted inorganic $PM_{2.5}$ in China in 2010 is most sensitive to NH_3 emissions in January and more sensitive to SO_2 and NO_x emissions in July. When national SO_2 and NO_x emissions reduce by 60% and 30%, respectively, the sensitivity of $PM_{2.5}$ to NH_3 emissions would decrease by 25% in winter, but sensitivity to further NO_x emission reductions would increase by nearly a factor of three. Although NH_3 remains to be the most sensitive one in winter, the relative difference between NH_3 and NO_x sensitivity decrease from one magnitude to a factor of three.

These co-benefits studies suggest that interactions between climate policy and end-of-pipe control policy as well as international cooperation should be considered when formulating new policy proposals. Health co-benefits of a moderate climate policy in China can potentially outweigh policy costs to households in 2030 even without considering a social cost of carbon (Tol et al., 2011). Co-benefits in terms of avoided premature mortalities from ozone reduction might be comparable in magnitude to those from $PM_{2.5}$ reduction, thus should not be neglected in future studies. Climate policy in China could also reduce a large number of air pollution related mortalities outside of China's borders. The avoided premature deaths in the US estimated here are 4-17% of those from domestic climate policy in the US (Shindell et al., 2016; Thompson et al., 2014; Y. Zhang et al., 2017). This co-benefits modeling framework could also be applied to other developing nations such as India.

China has been controlling SO_2 and NO_x emissions to mitigate air pollution, but the sensitivity study in Chapter 4 suggests that controlling NH_3 emissions in winter may be more effective in reducing $PM_{2.5}$, even when SO_2 and NO_x emissions decrease substantially. Earlier studies in the US (Pinder et al., 2007) showed that controlling NH_3 emissions could be cost-effective as well, but such control measures have not yet been implemented. Further research on the cost and feasibility of NH_3 control measures in China is highly needed. In addition, we found that when SO_2 and NO_x emissions decrease by 60% and 30%, respectively, sensitivity to further NO_x emission reductions would increase by nearly a factor of three. On the other hand, the marginal cost of NO_x emission reductions (either through end-of-pipe or climate policy) is also expected to increase with further emission reduction. Future studies that combine cost information and sensitivities calculated in this study could examine how the cost-effectiveness of NO_x control policies would evolve over time. A similar research in case of ozone in the US

found that nationwide NO_x emission reductions significantly increase the marginal benefits of NO_x reductions (Pappin et al., 2015). The methodology used in this work can also be applied to study the sensitivity of ozone to NO_x and VOCs emissions and cost-effective emissions control policies in China. As NO_x is the precursor of both $PM_{2.5}$ and ozone, optimized co-control of both pollutants should also be considered in future studies.

Meteorology is kept constant in all the studies of this thesis. Many previous studies have found that climate change could increase ozone and $PM_{2.5}$ concentrations in certain regions by altering natural emissions, chemistry, deposition, or transport (e.g. Jacob and Winner, 2009; Fiore et al., 2015). Therefore, climate policy may have additional air quality co-benefits by slowing down climate change. Co-benefits from this mechanism has been quantified to be smaller than those from emission reduction on global scales (West et al. 2013), but can still offset a significant fraction of policy costs in the US (Garcia-Menendez et al. 2015). Future research can be conducted to quantify its magnitude in China and how it compares with co-benefits from emission reductions. In addition, how climate change would affect the sensitivities of inorganic $PM_{2.5}$ to precursor emissions in Chapter 4 is of interest as well.

In conclusion, the proposed carbon policy in China has large air quality and health co-benefits in China that could potentially fully offset carbon policy cost in 2030. This policy also reduces a large number of air pollution related premature deaths in transboundary regions in 2030, and the avoided deaths in the US are several percent of those from domestic climate policy. To reduce the concentrations of inorganic $PM_{2.5}$ in China, controlling NH_3 emissions in the wintertime may be more effective than the proposed policies to control SO_2 and NO_x emissions. When national SO_2 and NO_x emissions reduce by 60% and 30%, the sensitivity of inorganic $PM_{2.5}$ to NH_3 emissions would decrease by 25% in winter, but sensitivity to further NO_x emission reductions would increase by nearly a factor of three. When formulating new air pollution control policies, China should consider its interaction with climate policy, feasible NH_3 emissions control measures, and possible chemical non-linearities that would affect the policy effectiveness over time.

Appendix A Supplemental Information for Chapter 2

Table A.1. Regional and sectoral aggregation in C-REM.

Regional	Sectoral (description in parenthesis)
Chinese mainland provinces	**Energy**
Anhui (AH)	COL (Coal mining and processing)
Beijing (BJ)	CRU (Crude petroleum products)
Chongqing (CQ)	GAS (Natural gas products)
Fujian (FJ)	OIL (Petroleum refining, coking, and nuclear fuels)
Guangdong (GD)	**Non-energy**
Gansu (GS)	AGR (Agricultural, forestry, and livestock)
Guangxi (GX)	CON (Construction)
Guizhou (GZ)	EIS (Energy intensive industries)
Henan (HA)	ELE (Electricity and heat)
Hubei (HB)	MAN (Other manufacturing industries)
Hebei (HE)	OMN (Metal/non-metal minerals mining)
Hainan (HI)	SER (Service)
Heilongjiang (HL)	TRN (Transport and post)
Hunan (HN)	WTR (Water supply)
Jilin (JL)	
Jiangsu (JS)	
Jiangxi (JX)	
Liaoning (LN)	
Inner Mongolia (NM)	
Ningxia (NX)	
Qinghai (QH)	
Sichuan (SC)	
Shandong (SD)	
Shanghai (SH)	
Shaanxi (SN)	
Shanxi (SX)	
Tianjin (TJ)	
Xinjiang (XJ)	
Yunnan (YN)	
Zhejiang (ZJ)	
Other regions	
United States	
Europe	
Other developed countries or regions*	
Rest of the world	

*It includes Australia, Canada, Japan, New Zealand, Singapore, South Korea, and Taiwan.

Table A.2. Sectoral mapping between REAS and C-REM.

Sectors in REAS*		Sectors in C-REM
AGR_FORE, AGR_FORE_FISH, AGRICULT, ENTERIC_FERMENTATI, FERT_PROD, FERTILIZER, FISHING, MANURE_MANAGEMENT, RICE_CULTIVATION	}	AGR
CRUDE_OIL	}	CRU
GAS_PROD, NATURAL_GAS, OTHER_GAS	}	GAS
DIESEL_OIL, KEROSENE, HEAVY_FUEL_OIL, MOTOR_GASOLINE, OTHER_HF, OTHER_LF	}	OIL
LIME, MINING, NON_MET_MINE	}	OMN
ADIPIC_ACID, ALUMINUM_ALUMINA, BRICKS, CEMENT, CERAMICS, COKE_OVENS, CRUDE_STEEL, IRON_AND_STEEL, NITRIC_ACID, NON_FERROUS_METAL, IRON_STEEL_OTHERS, NON_SPECIFIED, PIG_IRON, STEEL, SULPHRIC_ACID	}	EIS
POWER_PLANTS	}	ELE
AMMONIA, AMMONIUM_NITRATE, CHEM_PETRCHEM, CHEMICAL_IND, CHEMICAL_MATERIAL, CHEMICAL_PRODUCT, COPPER, DEGREASING, EXTRAC_PROC, FOOD, GLASS, INK_PROD, LEATHER, LEAD, MANUFACTURING, OTH_TRANSFORMATION, OTHER_PROD, OTHER_USAGE, OTHERS, PAINT_PROD, PAPER, PLASTIC, PRINTING, RUBBER, SMALL_INCIN TEXTILE, UREA, WASTE, WASTE_INCIN, ZINC	}	MAN
WASTE_WATER	}	WTR
CAR_EVAP, DOM_NAVI, RAILWAY_ETC, ROAD_BUSES, ROAD_H_TRUCKS, ROAD_L_TRUCKS, VEHICLE	}	TRN
COMM_PUB, COMMERCIAL, DRY_CLEANING	}	SER
DOM, PET_DOG, RESIDENT, ROAD_CARS, ROAD_MC, ROAD_OTHERS	}	c

*Full names and detailed description of sectors in REAS can be found in: http://www.nies.go.jp/REAS/.

Table A.3. Avoided mortality, policy cost, and health benefit by province in 2030 under the 4% Policy. References refer to alternative sources for underlying exposure-response relationships.

Province	Avoided Mortality			Consump. Loss*	Health Co-Benefit*	Net Benefit*
	ref [1]	ref [2]	ref [3]			
Beijing	1113	331	2443	5.0	9.4	4.4
Shanghai	558	23	175	2.9	4.5	1.6
Tianjin	691	299	2185	1.3	4.9	3.6
Jiangsu	2196	1053	7833	2.3	13.0	10.8
Zhejiang	3282	699	5240	8.3	20.7	12.5
Shandong	4692	2280	16860	1.3	23.0	21.8
Guangdong	10383	1196	8971	15.2	53.7	38.5
Liaoning	3878	1437	10745	-2.4	17.1	19.5
Fujian	4785	546	4106	1.3	22.3	21.1
Inner Mongolia	3181	1342	10100	11.2	18.5	7.3
Jilin	3616	1209	9070	0.3	15.2	14.8
Heilongjiang	5766	1129	8505	8.9	26.8	18.0
Chongqing	1503	1246	9171	3.1	8.5	5.3
Shaanxi	1451	1802	13449	7.8	11.2	3.4
Hebei	4637	2822	20853	-5.8	13.6	19.4
Hubei	3551	3005	22088	2.6	15.6	12.9
Hainan	1522	84	635	1.6	6.2	4.5
Shanxi	2906	2262	16701	25.4	33.1	7.7
Hunan	3635	3578	26335	5.0	17.1	12.1
Henan	3913	2525	18631	5.8	20.3	14.6
Ningxia	248	231	1736	0.7	1.6	0.9
Jiangxi	1873	1396	10421	-1.0	6.3	7.3
Qinghai	781	194	1466	0.5	3.0	2.6
Xinjiang	1465	158	1196	2.0	6.4	4.3
Guangxi	3224	2402	17893	1.9	12.8	10.9
Anhui	2041	1647	12213	4.5	11.1	6.5
Sichuan	5300	3096	22844	7.5	24.5	17.0
Gansu	1888	852	6404	0.8	6.5	5.7
Yunnan	6938	1303	9793	1.5	22.7	21.2
Guizhou	3442	2111	15560	5.6	14.8	9.2
National	94459	42258	313622	125.0	464.5	339.6

*Consumption loss, health co-benefit, and net benefit are reported in billion USD. Health co-benefit and net benefit are calculated using the exposure response function in Burnett et al. (2014) [1].

81
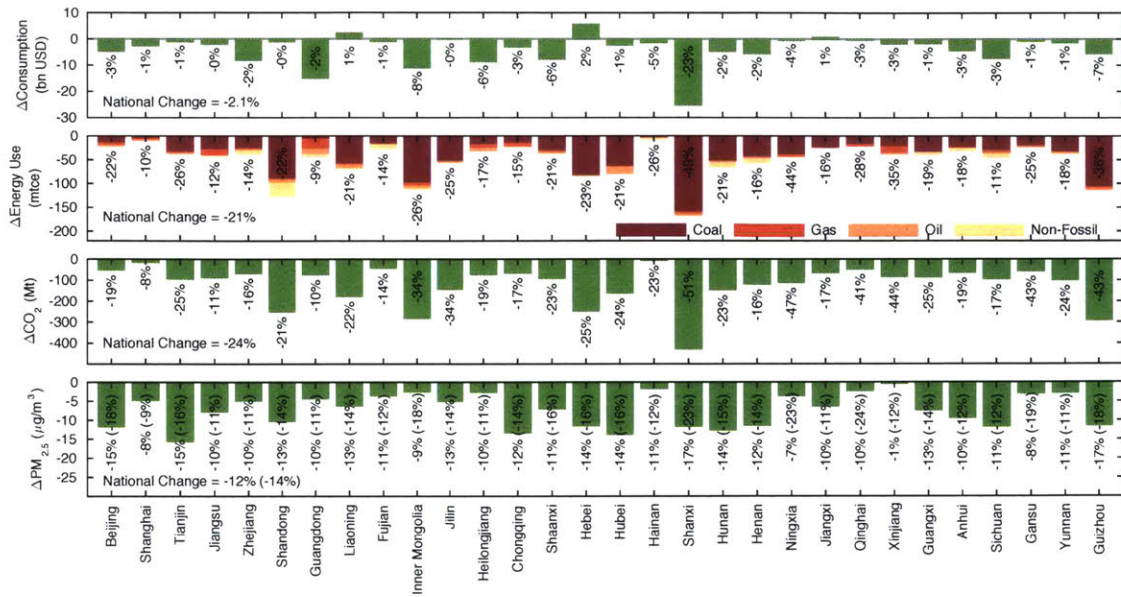
Figure A.1. Changes in multiple outcomes due to the 4 % Policy, compared to the No Policy scenario in 2030. From top to bottom: consumption, energy use, CO_2 emission, and population-weighted total $PM_{2.5}$ concentration. Numbers beside each bar represent percentage changes, and numbers inside the parentheses in the bottom panel are percentage changes in terms of anthropogenic $PM_{2.5}$.
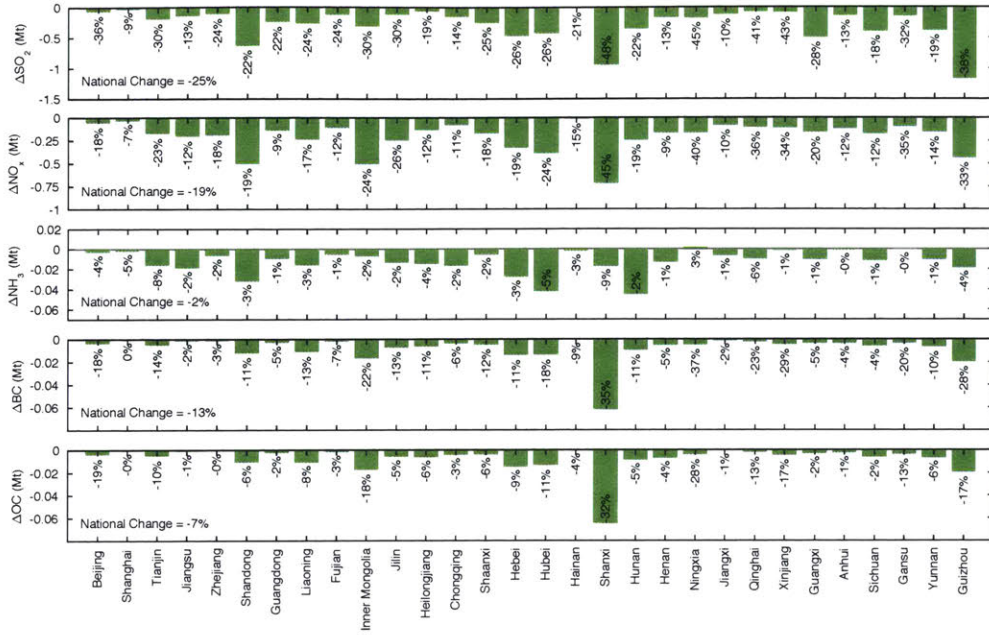
Figure A.2. Changes in precursor emissions due to the 4 % Policy, compared to the No Policy scenario in 2030. Numbers beside each bar represent percentage changes.
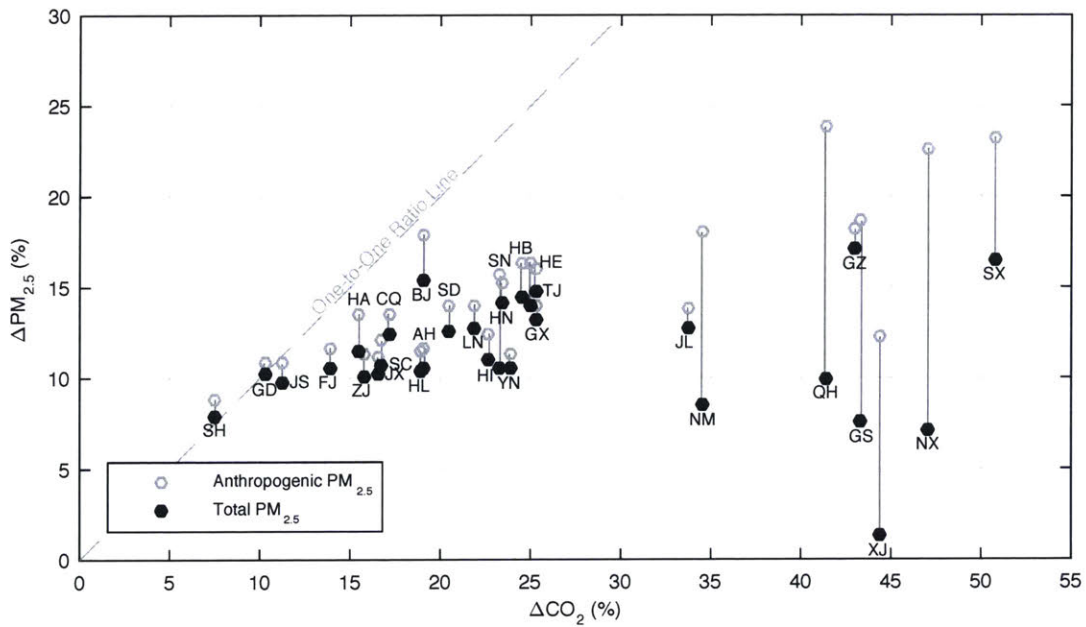
Figure A.3. Percentage changes of $PM_{2.5}$ vs. CO_2 due to the 4% Policy, compared to the No Policy scenario in 2030.

References

[1] Burnett, R. T.; Pope, C. A.; Ezzati, M.; Olives, C.; Lim, S. S.; Mehta, S.; Shin, H. H.; Singh, G.; Hubbell, B.; Brauer, M.; et al. An Integrated Risk Function for Estimating the Global Burden of Disease Attributable to Ambient Fine Particulate Matter Exposure. *Environmental Health Perspectives* **2014**, *122* (4), 397–403. https://doi.org/10.1289/ehp.1307049.

[2] Cao, J.; Yang, C.; Li, J.; Chen, R.; Chen, B.; Gu, D.; Kan, H. Association between Long-Term Exposure to Outdoor Air Pollution and Mortality in China: A Cohort Study. *Journal of Hazardous Materials* **2011**, *186* (2–3), 1594–1600. https://doi.org/10.1016/j.jhazmat.2010.12.036.

[3] Krewski, D. et al. Extended Follow-Up and Spatial Analysis of the American Cancer Society Study Linking Particulate Air Pollution and Mortality Report No. 140 (Health Effects Institute Research, 2009).

Bibliography

Anenberg, S. C.; West, J. J.; Fiore, A. M.; Jaffe, D. A.; Prather, M. J.; Bergmann, D.; Cuvelier, K.; Dentener, F. J.; Duncan, B. N.; Gauss, M.; et al. Intercontinental Impacts of Ozone Pollution on Human Mortality. *Environmental Science & Technology* **2009**, *43* (17), 6482–6487. https://doi.org/10.1021/es900518z.

Anenberg, S. C.; West, J. J.; Yu, H.; Chin, M.; Schulz, M.; Bergmann, D.; Bey, I.; Bian, H.; Diehl, T.; Fiore, A.; et al. Impacts of Intercontinental Transport of Anthropogenic Fine Particulate Matter on Human Mortality. *Air Quality, Atmosphere & Health* **2014**, *7* (3), 369–379. https://doi.org/10.1007/s11869-014-0248-9.

Ansari, A. S.; Pandis, S. N. Response of Inorganic PM to Precursor Concentrations. *Environmental Science & Technology* **1998**, *32* (18), 2706–2714. https://doi.org/10.1021/es971130j.

Arrow, K. J.; Debreu, G. Existence of an equilibrium for a competitive economy. *Econometrica* **1954**, 22, 265–290.

Aunan, K.; Fang, J.; Vennemo, H.; Oye, K.; Seip, H. M. Co-Benefits of Climate Policy—Lessons Learned from a Study in Shanxi, China. *Energy Policy* **2004**, *32* (4), 567–581. https://doi.org/10.1016/S0301-4215(03)00156-3.

Brown-Steiner, B.; Hess, P. Asian Influence on Surface Ozone in the United States: A Comparison of Chemistry, Seasonality, and Transport Mechanisms. *Journal of Geophysical Research* **2011**, *116* (D17), D17309. https://doi.org/10.1029/2011JD015846.

Burnett, R. T.; Pope, C. A.; Ezzati, M.; Olives, C.; Lim, S. S.; Mehta, S.; Shin, H. H.; Singh, G.; Hubbell, B.; Brauer, M.; et al. An Integrated Risk Function for Estimating the Global Burden of Disease Attributable to Ambient Fine Particulate Matter Exposure. *Environmental Health Perspectives* **2014**, *122* (4), 397–403. https://doi.org/10.1289/ehp.1307049.

Burnett, R.; Chen, H.; Szyszkowicz, M.; Fann, N.; Hubbell, B.; Pope, C. A.; Apte, J. S.; Brauer, M.; Cohen, A.; Weichenthal, S.; et al. Global Estimates of Mortality Associated with Long-Term Exposure to Outdoor Fine Particulate Matter. *Proceedings of the National Academy of Sciences* **2018**, *115* (38), 9592–9597. https://doi.org/10.1073/pnas.1803222115.

Cao, J.; Yang, C.; Li, J.; Chen, R.; Chen, B.; Gu, D.; Kan, H. Association between Long-Term Exposure to Outdoor Air Pollution and Mortality in China: A Cohort Study. *Journal of Hazardous Materials* **2011**, *186* (2–3), 1594–1600. https://doi.org/10.1016/j.jhazmat.2010.12.036.

Center for International Earth Science Information Network. *Gridded Population of the World* Version 3. 2005. http://sedac.ciesin.columbia.edu/data/ set/gpw-v3-population-count-future-estimates

Cheng, Y.; Zheng, G.; Wei, C.; Mu, Q.; Zheng, B.; Wang, Z.; Gao, M.; Zhang, Q.; He, K.; Carmichael, G.; et al. Reactive Nitrogen Chemistry in Aerosol Water as a Source of Sulfate during Haze Events in China. *Science Advances* **2016**, *2* (12), e1601530. https://doi.org/10.1126/sciadv.1601530.

China MEP. *Ambient Air Quality Standards* GB 3095–2012. 2012. http://english.mep.gov.cn/Resources/standards/Air_Environment/quality_standard1/201605/W020160 511506615956495.pdf

Chow, J. C.; Watson, J. G. Guideline on Speciated Particulate Monitoring. 291.

Dong, H.; Dai, H.; Dong, L.; Fujita, T.; Geng, Y.; Klimont, Z.; Inoue, T.; Bunya, S.; Fujii, M.; Masui, T. Pursuing Air Pollutant Co-Benefits of CO 2 Mitigation in China: A Provincial Leveled Analysis. *Applied Energy* **2015**, *144*, 165–174. https://doi.org/10.1016/j.apenergy.2015.02.020.

Driscoll, C. T.; Buonocore, J. J.; Levy, J. I.; Lambert, K. F.; Burtraw, D.; Reid, S. B.; Fakhraei, H.; Schwartz, J. US Power Plant Carbon Standards and Clean Air and Health Co-Benefits. *Nature Climate Change* **2015**, *5* (6), 535–540. https://doi.org/10.1038/nclimate2598.

Fiore, A. M.; Naik, V.; Spracklen, D. V.; Steiner, A.; Unger, N.; Prather, M.; Bergmann, D.; Cameron-Smith; P.J., Cionni; I., Collins, W.J.; Dalsøren, S. Global air quality and climate. *Chemical Society Reviews* **2012**, 41(19), 6663–6683.

Fisher, J. A.; Jacob, D. J.; Wang, Q.; Bahreini, R.; Carouge, C. C.; Cubison, M. J.; Dibb, J. E.; Diehl, T.; Jimenez, J. L.; Leibensperger, E. M.; et al. Sources, Distribution, and Acidity of Sulfate–Ammonium Aerosol in the Arctic in Winter–Spring. *Atmospheric Environment* **2011**, *45* (39), 7301–7318. https://doi.org/10.1016/j.atmosenv.2011.08.030.

Fountoukis, C.; Nenes, A. ISORROPIA II: A Computationally Efficient Thermodynamic Equilibrium Model for K^+–Ca^{2+}–Mg^{2+}–NH_4^+–Na^+–SO_4^{2-}–NO_3^-–Cl^-–H_2O Aerosols. *Atmospheric Chemistry and Physics* **2007**, 21.

Fu, T.-M.; Cao, J. J.; Zhang, X. Y.; Lee, S. C.; Zhang, Q.; Han, Y. M.; Qu, W. J.; Han, Z.; Zhang, R.; Wang, Y. X.; et al. Carbonaceous Aerosols in China: Top-down Constraints on Primary Sources and Estimation of Secondary Contribution. *Atmospheric Chemistry and Physics* **2012**, *12* (5), 2725–2746. https://doi.org/10.5194/acp-12-2725-2012.

Fu, X.; Wang, S.; Xing, J.; Zhang, X.; Wang, T.; Hao, J. Increasing Ammonia Concentrations Reduce the Effectiveness of Particle Pollution Control Achieved via SO_2 and NO_X Emissions Reduction in East China. *Environmental Science & Technology Letters* **2017**, *4* (6), 221–227. https://doi.org/10.1021/acs.estlett.7b00143.

Garcia-Menendez, F.; Saari, R. K.; Monier, E.; Selin, N. E. U.S. Air Quality and Health Benefits from Avoided Climate Change under Greenhouse Gas Mitigation. *Environmental Science & Technology* **2015**, *49* (13), 7580–7588. https://doi.org/10.1021/acs.est.5b01324.

Hammitt, J. K.; Robinson, L. A. The Income Elasticity of the Value per Statistical Life: Transferring Estimates between High and Low Income Populations. *Journal of Benefit-Cost Analysis* **2011**, *2* (01), 1–29. https://doi.org/10.2202/2152-2812.1009.

He, J.; Wang, H. *The Value of Statistical Life: A Contingent Investigation in China*; Policy Research Working Papers; The World Bank, 2010. https://doi.org/10.1596/1813-9450-5421.

He, K.; Lei, Y.; Pan, X.; Zhang, Y.; Zhang, Q.; Chen, D. Co-Benefits from Energy Policies in China. *Energy* **2010**, *35* (11), 4265–4272. https://doi.org/10.1016/j.energy.2008.07.021.

He, K.; Zhao, Q.; Ma, Y.; Duan, F.; Yang, F.; Shi, Z.; Chen, G. Spatial and Seasonal Variability of $PM_{2.5}$ Acidity at Two Chinese Megacities: Insights into the Formation of Secondary Inorganic Aerosols. *Atmospheric Chemistry and Physics* **2012**, *12* (3), 1377–1395. https://doi.org/10.5194/acp-12-1377-2012.

Heald, C. L.; Collett, J. L.; Lee, T.; Benedict, K. B.; Schwandner, F. M.; Li, Y.; Clarisse, L.; Hurtmans, D. R.; Van Damme, M.; Clerbaux, C.; et al. Atmospheric Ammonia and Particulate Inorganic Nitrogen over the United States. *Atmospheric Chemistry and Physics* **2012**, *12* (21), 10295–10312. https://doi.org/10.5194/acp-12-10295-2012.

Holt, J.; Selin, N. E.; Solomon, S. Changes in Inorganic Fine Particulate Matter Sensitivities to Precursors Due to Large-Scale US Emissions Reductions. *Environmental Science & Technology* **2015**, *49* (8), 4834–4841. https://doi.org/10.1021/acs.est.5b00008.

Huang, X.; Song, Y.; Li, M.; Li, J.; Huo, Q.; Cai, X.; Zhu, T.; Hu, M.; Zhang, H. A High-Resolution Ammonia Emission Inventory in China. *Global Biogeochemical Cycles* **2012**, *26* (1), GB1030. https://doi.org/10.1029/2011GB004161.

Institute for Health Metrics and Evaluation. *Global Burden of Disease Study 2010: Ambient Air Pollution Risk Model 1990–2010.* 2013. http://ghdx. healthdata.org/record/global-burden-disease-study-2010-gbd-2010-ambient- air-pollution-risk-model-1990-2010

IPCC. *2006 IPCC Guidelines for National Greenhouse Gas Inventories.* 2006.

Jacob, D. J.; Winner, D. A. Effect of climate change on air quality. *Atmospheric Environment* **2009**, 43(1), 51–63.

Jerrett, M.; Burnett, R. T.; Pope, C. A.; Ito, K.; Thurston, G.; Krewski, D.; Shi, Y.; Calle, E.; Thun, M. Long-Term Ozone Exposure and Mortality. *New England Journal of Medicine* **2009**, *360* (11), 1085–1095. https://doi.org/10.1056/NEJMoa0803894.

Jin, X.; Fiore, A. M.; Murray, L. T.; Valin, L. C.; Lamsal, L. N.; Duncan, B.; Folkert Boersma, K.; De Smedt, I.; Abad, G. G.; Chance, K.; et al. Evaluating a Space-Based Indicator of Surface Ozone-NO_x-VOC Sensitivity Over Midlatitude Source Regions and Application to Decadal Trends: Space-Based Indicator of O_3 Sensitivity. *Journal of Geophysical Research: Atmospheres* **2017**, *122* (19), 10,439-10,461. https://doi.org/10.1002/2017JD026720.

Karplus, V. J.; Rausch, S.; Zhang, D. Energy Caps: Alternative Climate Policy Instruments for China? *Energy Economics* **2016**, *56*, 422–431. https://doi.org/10.1016/j.eneco.2016.03.019.

Kharol, S. K.; Martin, R. V.; Philip, S.; Vogel, S.; Henze, D. K.; Chen, D.; Wang, Y.; Zhang, Q.; Heald, C. L. Persistent Sensitivity of Asian Aerosol to Emissions of Nitrogen Oxides. *Geophysical Research Letters* **2013**, *40* (5), 1021–1026. https://doi.org/10.1002/grl.50234.

Krewski, D. et al. *Extended Follow-Up and Spatial Analysis of the American Cancer Society Study Linking Particulate Air Pollution and Mortality* Report No. 140. Health Effects Institute Research. 2009.

Kurokawa, J.; Ohara, T.; Morikawa, T.; Hanayama, S.; Janssens-Maenhout, G.; Fukui, T.; Kawashima, K.; Akimoto, H. Emissions of Air Pollutants and Greenhouse Gases over Asian Regions during 2000–2008: Regional Emission Inventory in ASia (REAS) Version 2. *Atmospheric Chemistry and Physics* **2013**, *13* (21), 11019–11058. https://doi.org/10.5194/acp-13-11019-2013.

Lee, C. J.; Martin, R. V.; Henze, D. K.; Brauer, M.; Cohen, A.; Donkelaar, A. van. Response of Global Particulate-Matter-Related Mortality to Changes in Local Precursor Emissions. *Environmental Science & Technology* **2015**, *49* (7), 4335–4344. https://doi.org/10.1021/acs.est.5b00873.

Leibensperger, E. M.; Mickley, L. J.; Jacob, D. J.; Barrett, S. R. H. Intercontinental Influence of NOx and CO Emissions on Particulate Matter Air Quality. *Atmospheric Environment* **2011**, *45* (19), 3318–3324. https://doi.org/10.1016/j.atmosenv.2011.02.023.

Lelieveld, J.; Evans, J. S.; Fnais, M.; Giannadaki, D.; Pozzer, A. The Contribution of Outdoor Air Pollution Sources to Premature Mortality on a Global Scale. *Nature* **2015**, *525* (7569), 367–371. https://doi.org/10.1038/nature15371.

Li, J.; Wang, Z.; Akimoto, H.; Gao, C.; Pochanart, P.; Wang, X. Modeling Study of Ozone Seasonal Cycle in Lower Troposphere over East Asia. *Journal of Geophysical Research* **2007**, *112* (D22), D22S25. https://doi.org/10.1029/2006JD008209.

Li, M.; Zhang, D.; Li, C.-T.; Mulvaney, K. M.; Selin, N. E.; Karplus, V. J. Air Quality Co-Benefits of Carbon Pricing in China. *Nature Climate Change* **2018**, *8* (5), 398–403. https://doi.org/10.1038/s41558-018-0139-4.

Li, M.; Zhang, D.; Li, C. T.; Selin, N. E.; Karplus, V. J. Co-benefits of China's climate policy for air quality and human health in China and transboundary regions in 2030. Submitted to *Environmental Research Letters*.

Liang, C.-K.; West, J. J.; Silva, R. A.; Bian, H.; Chin, M.; Davila, Y.; Dentener, F. J.; Emmons, L.; Flemming, J.; Folberth, G.; et al. HTAP2 Multi-Model Estimates of Premature Human Mortality Due to Intercontinental Transport of Air Pollution and Emission Sectors. *Atmospheric Chemistry and Physics* **2018**, *18* (14), 10497–10520. https://doi.org/10.5194/acp-18-10497-2018.

Lin, W.; Xu, X.; Zhang, X.; Tang, J. Contributions of Pollutants from North China Plain to Surface Ozone at the Shangdianzi GAW Station. *Atmospheric Chemistry and Physics* **2008**, 10.

Luo, G.; Yu, F.; Schwab, J. Revised Treatment of Wet Scavenging Processes Dramatically Improves GEOS-Chem 12.0.0 Simulations of Nitric Acid, Nitrate, and Ammonium over the United States. *Geoscientific Model Development Discussions* **2019**, 1–18. https://doi.org/10.5194/gmd-2019-58.

Luo, X.; Caron, J.; Karplus, V. J.; Zhang, D.; Zhang, X. Interprovincial Migration and the Stringency of Energy Policy in China. *Energy Economics* **2016**, *58*, 164–173. https://doi.org/10.1016/j.eneco.2016.05.017.

Ma, Q.; Cai, S.; Wang, S.; Zhao, B.; Martin, R. V.; Brauer, M.; Cohen, A.; Jiang, J.; Zhou, W.; Hao, J.; et al. Impacts of Coal Burning on Ambient $PM_{2.5}$ Pollution in China. *Atmospheric Chemistry and Physics* **2017**, *17* (7), 4477–4491. https://doi.org/10.5194/acp-17-4477-2017.

Martin, R.V.; Fiore, A.M.; Van Donkelaar, A. Space-based diagnosis of surface ozone sensitivity to anthropogenic emissions. *Geophysical Research Letters* **2004**, 31(6), L06120.

McCollum, D. L.; Krey, V.; Riahi, K.; Kolp, P.; Grubler, A.; Makowski, M.; Nakicenovic, N. Climate Policies Can Help Resolve Energy Security and Air Pollution Challenges. *Climatic Change* **2013**, *119* (2), 479–494. https://doi.org/10.1007/s10584-013-0710-y.

Nam, K.-M.; Waugh, C. J.; Paltsev, S.; Reilly, J. M.; Karplus, V. J. Carbon Co-Benefits of Tighter SO2 and NOx Regulations in China. *Global Environmental Change* **2013**, *23* (6), 1648–1661. https://doi.org/10.1016/j.gloenvcha.2013.09.003.

Narayanan, G. B.; Aguiar, A.; McDougall, R. *Global Trade, Assistance, and Production: the GTAP 8 Data Base.* Center for Global Trade Analysis, Purdue University. 2012.

National Bureau of Statistics of China. *China Energy Statistical Yearbook 2008.* 2011.

National Bureau of Statistics of China. *China Statistical Database.* 2012.

National Bureau of Statistics of China. *The China Regional Input–Output Tables 2007.* 2011.

National Development and Reform Commission, Department of Climate Change. *China's Intended Nationally Defined Contribution (INDC): Enhanced Actions on Climate Change.* 2015.

Nemet, G. F.; Holloway, T.; Meier, P. Implications of Incorporating Air-Quality Co-Benefits into Climate Change Policymaking. *Environmental Research Letters* **2010**, *5* (1), 014007. https://doi.org/10.1088/1748-9326/5/1/014007.

Nielsen, C. P.; Ho, M. S. *Clearer Skies Over China.* MIT Press, Cambridge. 2013.

Pappin, A. J.; Mesbah, S. M.; Hakami, A.; Schott, S. Diminishing returns or compounding benefits of air pollution control? The case of NOx and ozone. *Environmental Science & Technology* **2015**, 49(16), 9548–9556.

Park, R. J. Natural and Transboundary Pollution Influences on Sulfate-Nitrate-Ammonium Aerosols in the United States: Implications for Policy. *Journal of Geophysical Research* **2004**, *109* (D15), D15204. https://doi.org/10.1029/2003JD004473.

Parry, I.; Veung, C.; Heine, D. How Much Carbon Pricing is in Countries' Own Interests? The Critical Role of Co-benefits. *Climate Change Economics* **2015**, *06* (04), 1550019. https://doi.org/10.1142/S2010007815500190.

Paulot, F.; Jacob, D. J. Hidden Cost of U.S. Agricultural Exports: Particulate Matter from Ammonia Emissions. *Environmental Science & Technology* **2014**, *48* (2), 903–908. https://doi.org/10.1021/es4034793.

Peng, W.; Yang, J.; Lu, X.; Mauzerall, D. L. Potential Co-Benefits of Electrification for Air Quality, Health, and CO2 Mitigation in 2030 China. *Applied Energy* **2018**, *218*, 511–519. https://doi.org/10.1016/j.apenergy.2018.02.048.

Pinder, R. W.; Adams, P. J.; Pandis, S. N. Ammonia Emission Controls as a Cost-Effective Strategy for Reducing Atmospheric Particulate Matter in the Eastern United States. *Environmental Science & Technology* **2007**, *41* (2), 380–386. https://doi.org/10.1021/es060379a.

Pye, H. O. T.; Liao, H.; Wu, S.; Mickley, L. J.; Jacob, D. J.; Henze, D. K.; Seinfeld, J. H. Effect of Changes in Climate and Emissions on Future Sulfate-Nitrate-Ammonium Aerosol Levels in the United States: Future Inorganic Aerosols in the U.S. *Journal of Geophysical Research: Atmospheres* **2009**, *114* (D1). https://doi.org/10.1029/2008JD010701.

Raftery, A. E.; Zimmer, A.; Frierson, D. M. W.; Startz, R.; Liu, P. Less than 2 °C Warming by 2100 Unlikely. *Nature Climate Change* **2017**, *7* (9), 637–641. https://doi.org/10.1038/nclimate3352.

RIT International. *Environmental Benefits Mapping and Analysis Program–Community Edition User's Manual.* 2015.

Rutherford, T. F. Applied general equilibrium modeling with MPSGE as a GAMS subsystem: an overview of the modeling framework and syntax. *Comput. Econ.* **1999**, 14, 1–46.

Saari, R. K.; Mei, Y.; Monier, E.; Garcia-Menendez, F. Effect of Health-Related Uncertainty and Natural Variability on Health Impacts and Cobenefits of Climate Policy. *Environmental Science & Technology* **2019**, *53* (3), 1098–1108. https://doi.org/10.1021/acs.est.8b05094.

Shah, V.; Jaeglé, L.; Thornton, J. A.; Lopez-Hilfiker, F. D.; Lee, B. H.; Schroder, J. C.; Campuzano-Jost, P.; Jimenez, J. L.; Guo, H.; Sullivan, A. P.; et al. Chemical Feedbacks Weaken the Wintertime Response of Particulate Sulfate and Nitrate to Emissions Reductions over the Eastern United States. *Proceedings of the National Academy of Sciences* **2018**, *115* (32), 8110–8115. https://doi.org/10.1073/pnas.1803295115.

Shen, L.; Mickley, L. J.; Leibensperger, E. M.; Li, M. Strong Dependence of U.S. Summertime Air Quality on the Decadal Variability of Atlantic Sea Surface Temperatures: *Geophysical Research Letters* **2017**, *44* (24), 12,527-12,535. https://doi.org/10.1002/2017GL075905.

Shindell, D. T.; Lee, Y.; Faluvegi, G. Climate and Health Impacts of US Emissions Reductions Consistent with 2 °C. *Nature Climate Change* **2016**, *6* (5), 503–507. https://doi.org/10.1038/nclimate2935.

Shindell, D.; Kuylenstierna, J. C. I.; Vignati, E.; van Dingenen, R.; Amann, M.; Klimont, Z.; Anenberg, S. C.; Muller, N.; Janssens-Maenhout, G.; Raes, F.; et al. Simultaneously Mitigating Near-Term Climate Change and Improving Human Health and Food Security. *Science* **2012**, *335* (6065), 183–189. https://doi.org/10.1126/science.1210026.

Sillman, S. The use of NO_y, H_2O_2, and HNO_3 as indicators for ozone-NO_x-hydrocarbon sensitivity in urban locations. *Journal of Geophysical Research: Atmospheres* **1995**, 100(D7), 14175–14188.

Song, S.; Gao, M.; Xu, W.; Sun, Y.; Worsnop, D. R.; Jayne, J. T.; Zhang, Y.; Zhu, L.; Li, M.; Zhou, Z.; et al. Possible Heterogeneous Chemistry of Hydroxymethanesulfonate (HMS) in Northern China Winter Haze. *Atmospheric Chemistry and Physics* **2019**, *19* (2), 1357–1371. https://doi.org/10.5194/acp-19-1357-2019.

Springmann, M.; Zhang, D.; Karplus, V. J. Consumption-Based Adjustment of Emissions-Intensity Targets: An Economic Analysis for China's Provinces. *Environmental and Resource Economics* **2015**, *61* (4), 615–640. https://doi.org/10.1007/s10640-014-9809-5.

Streets, D. G.; Bond, T. C.; Carmichael, G. R.; Fernandes, S. D.; Fu, Q.; He, D.; Klimont, Z.; Nelson, S. M.; Tsai, N. Y.; Wang, M. Q.; et al. An Inventory of Gaseous and Primary Aerosol Emissions in Asia in the Year 2000. *Journal of Geophysical Research: Atmospheres* **2003**, *108* (D21). https://doi.org/10.1029/2002JD003093.

Thompson, T. M.; Rausch, S.; Saari, R. K.; Selin, N. E. A Systems Approach to Evaluating the Air Quality Co-Benefits of US Carbon Policies. *Nature Climate Change* **2014**, *4* (10), 917–923. https://doi.org/10.1038/nclimate2342.

Tol, R. S. J. The Social Cost of Carbon. *Annual Review of Resource Economics* **2011**, *3* (1), 419–443. https://doi.org/10.1146/annurev-resource-083110-120028.

Turner, M. C.; Jerrett, M.; Pope, C. A.; Krewski, D.; Gapstur, S. M.; Diver, W. R.; Beckerman, B. S.; Marshall, J. D.; Su, J.; Crouse, D. L.; et al. Long-Term Ozone Exposure and Mortality in a Large Prospective Study. *American Journal of Respiratory and Critical Care Medicine* **2016**, *193* (10), 1134–1142. https://doi.org/10.1164/rccm.201508-1633OC.

United Nations, Department of Economic and Social Affairs, Population Division. *World Population Prospects: the 2015 Revision.* 2015.

US Energy Information Administration. *Quarterly Coal Report April–June 2017.* 2017.

US Environmental Protection Agency. *Air Pollutant Emissions Trends Data.* 2016. https://www.epa.gov/air-emissions-inventories/air-pollutant-emissions-trends-data

US EPA. *Guidelines for Preparing Economic Analyses.* 2014. https://yosemite.epa.gov/ee/epa/eerm.nsf/vwAN/EE-0568-50.pdf/$ le/EE-0568-50.pdf

van Donkelaar, A.; Martin, R. V.; Brauer, M.; Hsu, N. C.; Kahn, R. A.; Levy, R. C.; Lyapustin, A.; Sayer, A. M.; Winker, D. M. Global Estimates of Fine Particulate Matter Using a Combined Geophysical-Statistical Method with Information from Satellites, Models, and Monitors. *Environmental Science & Technology* **2016**, *50* (7), 3762–3772. https://doi.org/10.1021/acs.est.5b05833.

van Vuuren, D. P.; Edmonds, J.; Kainuma, M.; Riahi, K.; Thomson, A.; Hibbard, K.; Hurtt, G. C.; Kram, T.; Krey, V.; Lamarque, J.-F.; et al. The Representative Concentration Pathways: An Overview. *Climatic Change* **2011**, *109* (1–2), 5–31. https://doi.org/10.1007/s10584-011-0148-z.

Viscusi, W. K. in *Handbook of the Economics of Risk and Uncertainty* Vol. 1 (eds Machina, M. & Viscusi, W. K.) Elsevier, Amsterdam **2014**, 385–452.

Voorhees, A. S.; Wang, J.; Wang, C.; Zhao, B.; Wang, S.; Kan, H. Public Health Benefits of Reducing Air Pollution in Shanghai: A Proof-of-Concept Methodology with Application to BenMAP. *Science of The Total Environment* **2014**, *485–486*, 396–405. https://doi.org/10.1016/j.scitotenv.2014.03.113.

Vos, T.; Barber, R. M.; Bell, B.; Bertozzi-Villa, A.; Biryukov, S.; Bolliger, I.; Charlson, F.; Davis, A.; Degenhardt, L.; Dicker, D.; et al. Global, Regional, and National Incidence, Prevalence, and Years Lived with Disability for 301 Acute and Chronic Diseases and Injuries in 188 Countries, 1990–2013: A Systematic Analysis for the Global Burden of Disease Study 2013. *The Lancet* **2015**, *386* (9995), 743–800. https://doi.org/10.1016/S0140-6736(15)60692-4.

Walker, J. M.; Philip, S.; Martin, R. V.; Seinfeld, J. H. Simulation of Nitrate, Sulfate, and Ammonium Aerosols over the United States. *Atmospheric Chemistry and Physics* **2012**, *12* (22), 11213–11227. https://doi.org/10.5194/acp-12-11213-2012.

Wang, S. X.; Zhao, B.; Cai, S. Y.; Klimont, Z.; Nielsen, C. P.; Morikawa, T.; Woo, J. H.; Kim, Y.; Fu, X.; Xu, J. Y.; et al. Emission Trends and Mitigation Options for Air Pollutants in East Asia. *Atmospheric Chemistry and Physics* **2014**, *14* (13), 6571–6603. https://doi.org/10.5194/acp-14-6571-2014.

Wang, S.; Xing, J.; Jang, C.; Zhu, Y.; Fu, J. S.; Hao, J. Impact Assessment of Ammonia Emissions on Inorganic Aerosols in East China Using Response Surface Modeling Technique. *Environmental Science & Technology* **2011**, *45* (21), 9293–9300. https://doi.org/10.1021/es2022347.

Wang, T.; Wei, X. L.; Ding, A. J.; Poon, C. N.; Lam, K. S.; Li, Y. S.; Chan, L. Y.; Anson, M. Increasing Surface Ozone Concentrations in the Background Atmosphere of Southern China, 1994–2007. *Atmospheric Chemistry and Physics* **2009**, 11.

Wang, Y. X.; McElroy, M. B.; Jacob, D. J.; Yantosca, R. M. A Nested Grid Formulation for Chemical Transport over Asia: Applications to CO. *Journal of Geophysical Research: Atmospheres* **2004**, *109* (D22), n/a-n/a. https://doi.org/10.1029/2004JD005237.

Wang, Y.; Zhang, Q. Q.; He, K.; Zhang, Q.; Chai, L. Sulfate-Nitrate-Ammonium Aerosols over China: Response to 2000–2015 Emission Changes of Sulfur Dioxide, Nitrogen Oxides, and Ammonia. *Atmospheric Chemistry and Physics* **2013**, *13* (5), 2635–2652. https://doi.org/10.5194/acp-13-2635-2013.

Wang, Y.; Zhang, Q.; Jiang, J.; Zhou, W.; Wang, B.; He, K.; Duan, F.; Zhang, Q.; Philip, S.; Xie, Y. Enhanced Sulfate Formation during China's Severe Winter Haze Episode in January 2013 Missing from Current Models. *Journal of Geophysical Research: Atmospheres* **2014**, *119* (17), 10,425-10,440. https://doi.org/10.1002/2013JD021426.

Wang, Y.; Zhang, Y.; Hao, J.; Luo, M. Seasonal and Spatial Variability of Surface Ozone over China: Contributions from Background and Domestic Pollution. *Atmospheric Chemistry and Physics* **2011**, *11* (7), 3511–3525. https://doi.org/10.5194/acp-11-3511-2011.

Webster, M., Paltsev, S., Parsons, J., Reilly, M. J. & Jacoby, H. D. *Uncertainty in Greenhouse Gas Emissions and Costs of Atmospheric Stabilization* Report No. 165. MIT Joint Program on the Science and Policy of Global Change. 2008.

West, J. J.; Smith, S. J.; Silva, R. A.; Naik, V.; Zhang, Y.; Adelman, Z.; Fry, M. M.; Anenberg, S.; Horowitz, L. W.; Lamarque, J.-F. Co-Benefits of Mitigating Global Greenhouse Gas Emissions for Future Air Quality and Human Health. *Nature Climate Change* **2013**, *3* (10), 885–889. https://doi.org/10.1038/nclimate2009.

World Health Organization. *WHOSIS: Detailed Data Files of the WHO Mortality Database.* 2015. http://www.who.int/healthinfo/statistics/mortality_rawdata/en/

Xing, L.; Fu, T.-M.; Cao, J. J.; Lee, S. C.; Wang, G. H.; Ho, K. F.; Cheng, M.-C.; You, C.-F.; Wang, T. J. Seasonal and Spatial Variability of the OM/OC Mass Ratios and High Regional Correlation between Oxalic Acid and Zinc in Chinese Urban Organic Aerosols. *Atmospheric Chemistry and Physics* **2013**, *13* (8), 4307–4318. https://doi.org/10.5194/acp-13-4307-2013.

Xu, L.; Chen, X.; Chen, J.; Zhang, F.; He, C.; Zhao, J.; Yin, L. Seasonal Variations and Chemical Compositions of PM2.5 Aerosol in the Urban Area of Fuzhou, China. *Atmospheric Research* **2012**, *104–105*, 264–272. https://doi.org/10.1016/j.atmosres.2011.10.017.

Yang, G., Fan, S., Tang, J., Jin, S. and Meng, Z. Characteristic of surface ozone concentrations at Lin'an. *Res. of Environ. Sci.* **2008**, 21, 31–35 (in Chinese).

Zhang, D.; Rausch, S.; Karplus, V. J.; Zhang, X. Quantifying Regional Economic Impacts of CO_2 Intensity Targets in China. *Energy Economics* **2013**, *40*, 687–701. https://doi.org/10.1016/j.eneco.2013.08.018.

Zhang, D.; Springmann, M.; Karplus, V. J. Equity and Emissions Trading in China. *Climatic Change* **2016**, *134* (1–2), 131–146. https://doi.org/10.1007/s10584-015-1516-x.

Zhang, L.; Jacob, D. J.; Boersma, K. F.; Jaffe, D. A.; Olson, J. R.; Bowman, K. W.; Worden, J. R.; Thompson, A. M.; Avery, M. A.; Cohen, R. C.; et al. Transpacific Transport of Ozone Pollution and the Effect of Recent Asian Emission Increases on Air Quality in North America: An Integrated Analysis Using Satellite, Aircraft, Ozonesonde, and Surface Observations. *Atmospheric Chemistry and Physics* **2008**, 20.

Zhang, Q.; Jiang, X.; Tong, D.; Davis, S. J.; Zhao, H.; Geng, G.; Feng, T.; Zheng, B.; Lu, Z.; Streets, D. G.; et al. Transboundary Health Impacts of Transported Global Air Pollution and International Trade. *Nature* **2017**, *543* (7647), 705–709. https://doi.org/10.1038/nature21712.

Zhang, R.; Jing, J.; Tao, J.; Hsu, S.-C.; Wang, G.; Cao, J.; Lee, C. S. L.; Zhu, L.; Chen, Z.; Zhao, Y.; et al. Chemical Characterization and Source Apportionment of $PM_{2.5}$ in Beijing: Seasonal Perspective. *Atmospheric Chemistry and Physics* **2013**, *13* (14), 7053–7074. https://doi.org/10.5194/acp-13-7053-2013.

Zhang, X. Y.; Wang, Y. Q.; Niu, T.; Zhang, X. C.; Gong, S. L.; Zhang, Y. M.; Sun, J. Y. Atmospheric Aerosol Compositions in China: Spatial/Temporal Variability, Chemical Signature, Regional Haze Distribution and Comparisons with Global Aerosols. *Atmospheric Chemistry and Physics* **2012**, *12* (2), 779–799. https://doi.org/10.5194/acp-12-779-2012.

Zhang, X.; Karplus, V. J.; Qi, T.; Zhang, D.; He, J. Carbon Emissions in China: How Far Can New Efforts Bend the Curve? *Energy Economics* **2016**, *54*, 388–395. https://doi.org/10.1016/j.eneco.2015.12.002.

Zhang, Y.; Smith, S. J.; Bowden, J. H.; Adelman, Z.; West, J. J. Co-Benefits of Global, Domestic, and Sectoral Greenhouse Gas Mitigation for US Air Quality and Human Health in 2050. *Environmental Research Letters* **2017**, *12* (11), 114033. https://doi.org/10.1088/1748-9326/aa8f76.

Zhao, B.; Wu, W.; Wang, S.; Xing, J.; Chang, X.; Liou, K.-N.; Jiang, J. H.; Gu, Y.; Jang, C.; Fu, J. S.; et al. A Modeling Study of the Nonlinear Response of Fine Particles to Air Pollutant Emissions in the Beijing–Tianjin–Hebei Region. *Atmospheric Chemistry and Physics* **2017**, *17* (19), 12031–12050. https://doi.org/10.5194/acp-17-12031-2017.

Zhao, P. S.; Dong, F.; He, D.; Zhao, X. J.; Zhang, X. L.; Zhang, W. Z.; Yao, Q.; Liu, H. Y. Characteristics of Concentrations and Chemical Compositions for $PM_{2.5}$ in the Region of Beijing, Tianjin, and Hebei, China. *Atmospheric Chemistry and Physics* **2013**, *13* (9), 4631–4644. https://doi.org/10.5194/acp-13-4631-2013.

Zhao, Y.; Zhang, J.; Nielsen, C. P. The Effects of Energy Paths and Emission Controls and Standards on Future Trends in China's Emissions of Primary Air Pollutants. *Atmospheric Chemistry and Physics* **2014**, *14* (17), 8849–8868. https://doi.org/10.5194/acp-14-8849-2014.

Zhao, Y.; Zhang, J.; Nielsen, C. P. The Effects of Recent Control Policies on Trends in Emissions of Anthropogenic Atmospheric Pollutants and CO_2; in China. *Atmospheric Chemistry and Physics* **2013**, *13* (2), 487–508. https://doi.org/10.5194/acp-13-487-2013.

Zheng, B.; Tong, D.; Li, M.; Liu, F.; Hong, C.; Geng, G.; Li, H.; Li, X.; Peng, L.; Qi, J.; et al. Trends in China's Anthropogenic Emissions since 2010 as the Consequence of Clean Air Actions. *Atmospheric Chemistry and Physics* **2018**, *18* (19), 14095–14111. https://doi.org/10.5194/acp-18-14095-2018.

Zhou, D. *China Sustainable Energy Scenarios in 2020.* China Environmental Science Press. 2003.